

# Measurement and parameterization of aerodynamic roughness length variations at Haut Glacier d'Arolla, Switzerland

Ben W. BROCK,<sup>1</sup> Ian C. WILLIS,<sup>2</sup> Martin J. SHARP<sup>3</sup>

<sup>1</sup>*Department of Geography, University of Dundee, Dundee DD1 4HN, UK  
E-mail: b.w.brock@dundee.ac.uk*

<sup>2</sup>*Scott Polar Research Institute, Department of Geography, University of Cambridge, Lensfield Road, Cambridge CB2 1ER, UK*

<sup>3</sup>*Department of Earth and Atmospheric Sciences, University of Alberta, Edmonton, Alberta T6G 2E3, Canada*

**ABSTRACT.** Spatial and temporal variations in aerodynamic roughness length ( $z_0$ ) on Haut Glacier d'Arolla, Switzerland, during the 1993 and 1994 ablation seasons are described, based on measurements of surface microtopography. The validity of the microtopographic  $z_0$  measurements is established through comparison with independent vertical wind profile  $z_0$  measurements over melting snow, slush and ice. The  $z_0$  variations are explained through correlation and regression analyses, using independent measurements of meteorological and surface variables, and parameterizations are developed to calculate  $z_0$  variations for use in surface energy balance melt models. Several independent variables successfully explain snow  $z_0$  variation through their correlation with increasing surface roughness, caused by ablation hollow formation, during snow melt. Non-linear parameterizations based on either accumulated melt or accumulated daily maximum temperatures since the most recent snowfall explain over 80% of snow  $z_0$  variation. The  $z_0$  following a fresh snowfall on an ice surface is parameterized based on relationships with the underlying ice  $z_0$ , snow depth and accumulated daily maximum temperatures. None of the independent variables were able to successfully explain ice  $z_0$  variation. Although further comparative studies are needed, the results lend strong support to the microtopographic technique of measuring  $z_0$  over melting glacier surfaces.

## 1. INTRODUCTION AND AIMS

The aerodynamic roughness length,  $z_0$ , defined as the height above a surface at which the extrapolated horizontal wind speed profile reaches zero, is an important control on the rate of turbulent heat transfer between a glacier surface and the air above it (Paterson, 1994; Oerlemans, 2001; Greuell and Genthon, 2004). On most glaciers the turbulent sensible and turbulent latent heat fluxes are significant sources of melt energy and, in maritime environments, are often the dominant source (Ishikawa and others, 1992; Willis and others, 2002). Thus,  $z_0$  variations need to be included in calculations of glacier surface melt rates (Brock and others, 2000), snowmelt runoff models (Samuelsson and others, 2003) and estimations of glacier mass balance and sea level changes under climatic warming scenarios (Braithwaite, 1995).

Little is known about the controls on spatial and temporal patterns of  $z_0$  variation on glaciers and it has been difficult to incorporate their effects into numerical surface melt models at the glacier-wide scale (e.g. Arnold and others, 1996; Hock and Holmgren, 1996; Brock and others, 2000; Klok and Oerlemans, 2002). To address these problems this study aims to: (i) monitor spatial and temporal variations in  $z_0$ , and several independent variables which may be used to explain them, across a glacier throughout an ablation season; (ii) identify which independent variables best explain  $z_0$  variations and (iii) develop regression-based parameterizations which can be used to calculate  $z_0$  in numerical surface-melt models.

The lack of systematic monitoring of  $z_0$  variations on glaciers stems partly from the difficulty of recording  $z_0$  at a large number of different sites, since techniques based on measurement of airflow in the surface atmospheric bound-

ary layer (SABL) require long periods of monitoring to generate a single  $z_0$  value. In order to monitor  $z_0$  variations across a glacier over an ablation season, measurements of surface microtopography must be used instead. However, the reliability of  $z_0$  measurements based on microtopographic methods has been questioned (Stull, 1988; Wieringa, 1993) and further verification through comparison with more established methods is needed (Smeets and others, 1999; Denby and Greuell, 2000). Thus, this study also tests the reliability of microtopographic  $z_0$  measurements through comparison with independent wind profile measurements of  $z_0$  over snow, slush and ice surfaces.

## 2. BACKGROUND

### 2.1. Theory: turbulent flux measurements over glacier surfaces

Calculations of turbulent sensible and latent heat fluxes between a glacier surface and the air above it are commonly made using the 'bulk' aerodynamic method, which assumes airflow in the SABL is turbulent and fully adjusted to the underlying terrain (e.g. Munro, 1990; Ishikawa and others, 1992; Van de Wal and others, 1992; Hock and Holmgren, 1996; Hock and Noetzli, 1997; Brock and others, 2000). Provided the influence of atmospheric stability is accounted for, this method is the most appropriate on sloping glacier surfaces where the wind speed maxima are within a few metres of the surface (Denby and Greuell, 2000). Its principal advantage is that measurements of horizontal wind speed, temperature and humidity need only be made at one height (usually 1 or 2 m) above the surface, as long as the  $z_0$  of the glacier surface in question is known. The value of  $z_0$  can be combined with a surface-renewal model

**Table 1(a).** Published aerodynamic roughness lengths recorded over mid- and low-latitude glaciers. The measurement method is indicated by letter as follows: e – eddy covariance; m – microtopographic; p – wind profile; r – residual in closed energy balance. Where available, the 1 standard deviation range is given in brackets after the mean  $z_0$  value

| $z_0$ ( $10^{-3}$ m) | Surface type (method)                | Author                         |
|----------------------|--------------------------------------|--------------------------------|
| Snow surfaces        |                                      |                                |
| 0.2                  | Fresh snow (p)                       | Poggi, 1977                    |
| 0.9                  | Glacier snow (p)                     | Wendler and Streten, 1969      |
| 0.9                  | Glacier snow (p)                     | Wendler and Weller, 1974       |
| 1–12                 | Rough snow (p)                       | Jackson and Carroll, 1978      |
| 1.3–2.0              | Glacier snow (p)                     | Greuell and Smeets, 2001       |
| 1.9                  | Seasonal snow (e, p)                 | Plüss and Mazzoni, 1994        |
| 2                    | Glacier snow (p)                     | Obleitner, 2000                |
| 2.5                  | Glacier snow (p)                     | Sverdrup, 1936                 |
| 4.0                  | Seasonal snow (p)                    | Moore and Owens, 1984          |
| 4                    | Tropical glacier wet season snow (r) | Wagnon and others, 1999        |
| 4.4                  | Melting snow (e, p)                  | Plüss and Mazzoni, 1994        |
| 5.0                  | Glacier snow (m)                     | Föhn, 1973                     |
| 5.0                  | Seasonal snow (m)                    | Price, 1977                    |
| 6.0                  | Glacier snow (m)                     | Munro, 1989                    |
| 14                   | Ablation hollows (p)                 | Hay and Fitzharris, 1988       |
| 30                   | Tropical glacier snow penitentes (r) | Wagnon and others, 1999        |
| Ice surfaces         |                                      |                                |
| 0.1                  | Glacier ice (p)                      | Grainger and Lister, 1966      |
| 0.1 (0.06–0.2)       | Glacier ice (e)                      | Smeets and others, 1998        |
| 0.7–2.5              | Glacier ice (e, m)                   | Munro, 1989                    |
| 1                    | Glacier ice (p)                      | Poggi, 1977                    |
| 1                    | Glacier ice (p)                      | Denby and Snellen, 2002        |
| 1.1                  | Glacier ice (p)                      | Schieb, 1962                   |
| 1.2–5.8              | Glacier ice (p)                      | Greuell and Smeets, 2001       |
| 1.3                  | Glacier ice (p)                      | Hogg and others, 1982          |
| 1.3–5.0              | Glacier ice (p)                      | Van de Wal and others, 1992    |
| 1.4 (1.0–2.2)        | Glacier ice (p)                      | Denby and Smeets, 2000         |
| 1.5                  | Glacier ice (p)                      | Hoinkes and Untersteiner, 1952 |
| 1.6 (1.0–2.8)        | Glacier ice (p)                      | Denby and Smeets, 2000         |
| 1.7                  | Glacier ice (p)                      | Hoinkes, 1953                  |
| 1.8                  | Glacier ice (p)                      | Streten and Wendler, 1968      |
| 2.0                  | Glacier ice (p)                      | Untersteiner, 1957             |
| 2.4                  | Glacier ice (p)                      | Wendler and Weller, 1974       |
| 2.4–2.7              | Glacier ice (p)                      | Ishikawa and others, 1992      |
| 5.8 (5.5–6.9)        | Glacier ice (p)                      | Martin, 1975                   |
| 3–15                 | Rough glacier ice (e, m, p)          | Smeets and others, 1999        |
| 20–80                | Very rough glacier ice (e, m, p)     | Smeets and others, 1999        |
| 50                   | Very rough glacier ice (p)           | Obleitner, 2000                |

(Brutseart, 1975; Andreas, 1987) to determine the roughness lengths of temperature and humidity, also required in the flux calculations (Denby and Greuell, 2000; Denby and Snellen, 2002).

The accuracy of the bulk method is dependent on the accuracy with which  $z_0$  can be specified. An order of magnitude increase in  $z_0$  will more than double the value of the turbulent fluxes (Brock and others, 2000) and an error in  $z_0$  of this magnitude is more significant to the turbulent flux calculation than neglect of atmospheric stability (Braithwaite, 1995). Aerodynamic roughness values recorded over melting glacier surfaces vary over three orders of magnitude, in the 0.1 to 10 mm range (Table 1a). At high latitudes, the recorded  $z_0$  range is five orders of magnitude from 0.001 to 10 mm (Table 1b). Often  $z_0$  is not measured in glacier energy balance studies and, due to the lack of a suitable parameterization scheme, a published value from another study, which may not necessarily be appropriate, must be used instead.

## 2.2. Controls on $z_0$ variation on glaciers

Under the normally turbulent flow conditions over melting snow and ice surfaces (Andreas, 1987),  $z_0$  depends solely on the dimensions, form and density distribution of surface roughness elements (Oke, 1987; Stull, 1988). The value of  $z_0$  increases with increasing height, surface area and density of surface roughness elements, until the ratio of the silhouette area (upwind face of elements) to unit ground area covered by each element, reaches 0.4, when a transition to 'skimming' flow occurs (Oke, 1987; Garratt, 1992) and  $z_0$  begins to decrease.

Over mid-latitude glaciers,  $z_0$  values recorded over smooth fresh snow surfaces are at the 0.1 mm scale, but lower values at the 0.01, or even 0.001 mm, scale have been recorded on snow over polar glaciers and ice sheets (Table 1b). Values reported for melting snow surfaces are in the 1 to 10 mm range, due to the development of ablation hollows and other microtopographical features in the snow

**Table 1(b).** Published aerodynamic roughness lengths recorded over high-latitude glaciers and ice sheets. The measurement method is indicated by letter as follows: e – eddy covariance; m – microtopographic; p – wind profile; r – residual in closed energy balance. Where available, the 1 standard deviation range is given in brackets after the mean  $z_0$  value

| $z_0$ ( $10^{-3}$ m) | Surface type (method)                | Author                                  |
|----------------------|--------------------------------------|---|
| Snow surfaces        |                                      |   |
| 0.004–0.15           | Antarctic plateau snow (e)           | Inoue, 1989                             |
| 0.04–0.05            | Polar glacier, spring snow (m)       | Arnold and Rees, 2003                   |
| 0.05–0.06            | Antarctic ice shelf snow (e)         | King and Anderson, 1994                 |
| 0.084                | Antarctic smooth snow (p)            | Bintanja and Van den Broeke, 1994, 1995 |
| 0.1                  | Antarctic snow field (p)             | Liljequist, 1954                        |
| 0.1                  | Antarctic Peninsula summer snow (r)  | Schneider, 1999                         |
| 0.11                 | Antarctic ice-shelf snow (e)         | King, 1990                              |
| 0.15 (0.1–0.21)      | Storglaciären snow (p)               | Hock and Holmgren, 1996                 |
| 0.2–0.3              | Polar glacier summer snow (m)        | Arnold and Rees, 2003                   |
| 0.3 (0.07–3.8)       | Antarctic summer snow (e)            | Grönlund and others, 2002               |
| 0.55–0.75            | Antarctic rough snow (p)             | Bintanja and Van den Broeke, 1994, 1995 |
| 0.9                  | Polar ice cap snow (p)               | Holmgren, 1971                          |
| 1                    | Antarctic summer snow (p)            | Bintanja, 2000                          |
| 6.8 (5.4–8.2)        | Greenland melting snow (p)           | Grainger and Lister, 1966               |
| 11 (8.5–13.5)        | Greenland sastrugi, early summer (p) | Grainger and Lister, 1966               |
| Ice surfaces         |                                      |   |
| 0.007                | Antarctic blue ice (p)               | Bintanja and Van den Broeke, 1994, 1995 |
| 0.1 (0.08–0.12)      | Storglaciären smooth ice (p)         | Grainger and Lister, 1966               |
| 0.1                  | Greenland ice (p)                    | Meesters and others, 1997               |
| 0.1                  | Antarctic blue ice (p)               | Bintanja, 2000, 2001                    |
| 0.17                 | Greenland, smooth ice (p)            | Ambach, 1963                            |
| 0.6–0.7              | Polar glacier ice (m)                | Arnold and Rees, 2003                   |
| 0.8–40               | Greenland ice (p)                    | Duynkerke and Van den Broeke, 1994      |
| 1.0                  | Greenland ice (p)                    | Van de Wal and Russel, 1994             |
| 1.8                  | Greenland ice (p)                    | Ambach, 1963                            |
| 2.2                  | Greenland ice (p)                    | Ambach, 1977                            |
| 2.7 (2.1–3.5)        | Storglaciären ice (p)                | Hock and Holmgren, 1996                 |
| 4.0 (2.4–5.6)        | Greenland early summer ice           | Grainger and Lister, 1966               |
| 4.4                  | Devon Island ice (p)                 | Keeler, 1964                            |
| 5.0 (1.9–8.1)        | Greenland mid-summer ice             | Grainger and Lister, 1966               |
| 5.7 (4.2–7.2)        | Greenland late-summer ice            | Grainger and Lister, 1966               |
| 5.8 (4.3–7.3)        | Hummocked glacier ice (p)            | Grainger and Lister, 1966               |
| 6.7                  | Canadian Arctic ice (p)              | Havens and others, 1965                 |

surface, with extremely high  $z_0$  values inferred for snow penitentes (Table 1).

On melting ice surfaces, dirt cones and boulder tables caused by surface insulation, and cryoconites and other features resulting from local melt differentials, create small-scale morphological features. Ice strain also creates surface morphology, e.g. crevasses and longitudinal foliae, which may enlarge through enhanced ablation along darker albedo bands. Correspondingly, while  $z_0$  values recorded over smooth ice are at the 0.1 mm scale, the majority of  $z_0$  values recorded on melting glacier ice are in the 1–10 mm scale range (Table 1). The very large  $z_0$  values recorded by Smeets and others (1999) and Obleitner (2000) relate to an area with very large roughness elements of 1–2 m height in the ablation zone of Breidamerkurjökull, Iceland (Table 1a), while extremely low  $z_0$  values are reported over Antarctic blue ice (Table 1b).

Smeets and others (1999) observed  $z_0$  to increase from a few millimetres to several tens of millimetres over the ablation season at Breidamerkurjökull in response to the growth of ice roughness elements from the 0.1 to 1 m scale. Similarly, Arnold and Rees (2003) recorded an increase in snow  $z_0$  from 0.04–0.05 mm to 0.2–0.3 mm between spring

and midsummer at midre Lovénbreen on Svalbard, with development of ablation hollows in the snow surface. In the ablation zone of the Greenland Ice Sheet, Grainger and Lister (1966) observed  $z_0$  to decrease from 11 to 6.8 mm, then to 5.8 mm, with changes in surface material from coarse snow sastrugi to melting snow and finally to rough ice. In contrast, Denby and Smeets (2000) and Greuell and Smeets (2001) recorded no variation in ice  $z_0$  over several months of measurements at Breidamerkurjökull, Iceland and Pasterze Glacier, Austria, respectively, which corresponded with no visible changes to the roughness of the surface. Similarly, Grainger and Lister (1966) reported no significant change in ice  $z_0$  in the lower ablation zone of the Greenland ice sheet over an ablation season. Overall, therefore, it is unclear whether there is a typical pattern of  $z_0$  evolution over glaciers during the ablation season.

The value of  $z_0$  varies with wind direction over irregularly shaped obstacles, e.g. sastrugi (Jackson and Carroll, 1978; Inoue, 1989; King and Anderson, 1994). For many glaciers wind direction is dominated by katabatic flows and topographic control, and is fairly constant (Greuell and others, 1997; Strasser and others, 2004). Therefore, dependence of

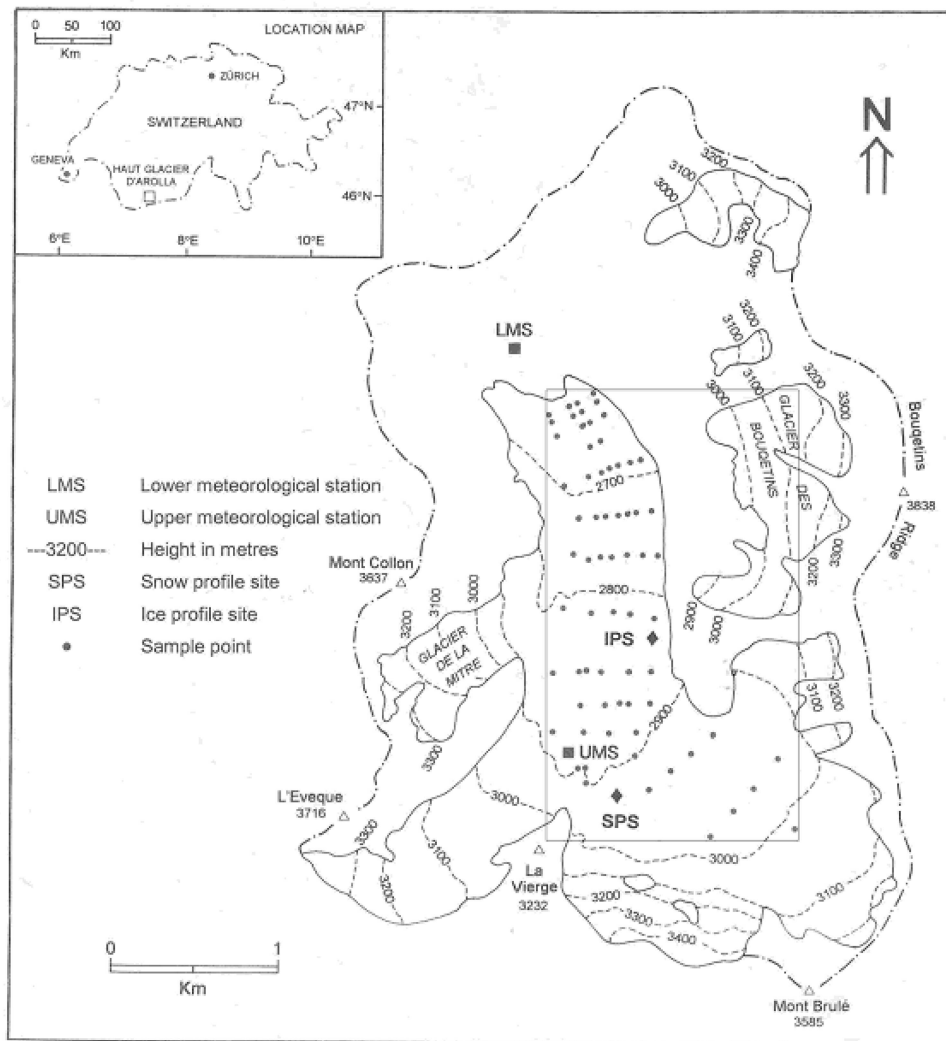


Fig. 1. Site map of Haut Glacier d'Arolla. The rectangle encloses the area of the glacier displayed in Figure 3.

$z_0$  on wind direction may not be of great significance to turbulent flux calculations in most cases.

Only a few of the studies quoted in Table 1 indicate the range of uncertainty in  $z_0$  measurements; in most cases a mean value is quoted. The most accurate values are likely to be obtained from Antarctic studies, where long homogenous fetch and a relatively deep SABL are favourable to  $z_0$  measurement using sonic anemometers. The vertical profile measurements carry greater uncertainty due to problems of sloping surfaces, atmospheric stability in the surface layer and difficulty in defining the base level for instruments on an uneven glacier surface (Morris, 1989; Smeets and others, 1999).

### 2.3. Measurement of $z_0$

Direct measurement of  $z_0$  is possible, using eddy covariance instruments, such as sonic anemometers, which respond to vertical wind velocity fluctuations on an instantaneous basis. However, these instruments are difficult to deploy on valley glaciers where the surface layer is thin and the instruments are prone to failure and damage (e.g. Munro, 1989; Plüss and Mazzoni, 1994; Smeets and others, 1999). Furthermore, the need for careful setting and calibration of the instruments, and long measurement periods mean this method is

unsuitable for measuring  $z_0$  at a large number of sites across a glacier.

The standard method is to derive  $z_0$  from the vertical profiles of horizontal wind speed and air temperature, using measurements at two or more heights in the SABL. The logarithmic wind speed profile can be adjusted for surface layer stability, using Monin–Obukhov similarity theory, enabling  $z_0$  to be found (e.g. Munro, 1989; Bintanja and Van den Broeke, 1994; Plüss and Mazzoni, 1994; Denby and Smeets, 2000; Obleitner, 2000; Greuell and Smeets, 2001). The instrumentation is more robust than for the eddy covariance method, and hence more suited to measurement over glaciers, but the calculation of  $z_0$  is very sensitive to errors in the instrument heights. A height error of just 0.1 m may change  $z_0$  by an order of magnitude, but defining the zero-reference plane for the instruments can prove difficult on a rough glacier surface (Munro, 1989; Smeets and others, 1999). A further problem is the shallow and variable nature of the SABL over mid-latitude glaciers, which may be shallower than the measurement heights (Grainger and Lister, 1966; Munro and Davies, 1977; Morris, 1989; Denby and Greuell, 2000; Arck and Scherer, 2002). Therefore, long measurement periods are needed to obtain the mean and standard error of the  $z_0$  value (Wieringa, 1993) and hence

the vertical profile method is also unsuitable for recording  $z_0$  at a large number of sites across a glacier.

Several workers have sought to overcome the  $z_0$  measurement problem through microtopographic measurements of the glacier surface (e.g. Föhn, 1973; Price, 1977; Munro, 1989; Arnold and Rees, 2003). Several relationships between surface roughness element geometry and  $z_0$  have been proposed, but it is the empirical relationship of Lettau (1969) which has gained widest acceptance in glacial and other studies:

$$z_0 = 0.5h^* \left( \frac{S}{S} \right) \quad (1)$$

in which  $h^*$  is the average vertical extent, or effective obstacle height, of the roughness elements;  $s$  is the silhouette area (area of upwind face of an average element) and  $S$  is the unit ground area occupied by each element.

The two main challenges for the microtopographic approach are to describe the surface roughness elements and to obtain a representative sample for accurate modelling of the glacier surface element dimensions (Munro, 1989; Smeets and others, 1999). A sampling method for Equation (1) suitable for glaciers was developed by Munro (1989, 1990). The only measurements required are of the variation of surface elevation made at regular intervals relative to a horizontal reference, in a plane perpendicular to the prevailing wind;  $h^*$  is calculated as twice the standard deviation of the elevations, with the mean elevation set to zero. The number of continuous groups of positive height deviations above the mean elevation defines the frequency,  $f$ , of roughness elements and the width of a typical element is defined as the length of the traverse,  $X$ , divided by  $2f$ . Equation (1) is solved by substituting  $s = h^*X/2f$  and  $S = (X/f)^2$ . Despite the simplification of surface element form, the estimation of the silhouette area of the elements using this approach is only  $\sim 12\%$  different from its true value (Munro, 1989).

Microtopographic  $z_0$  measurements have been independently verified using eddy correlation instruments at Peyto Glacier by Munro (1989) and with independent profile and eddy covariance measurements at Breidamerkurjökull (Smeets and others, 1999). However, these comparative measurements were limited to rough ice surfaces. Snow surfaces generally have a fairly isotropic distribution of roughness elements, but the applicability of the microtopographic method to anisotropic ice surfaces has been questioned (Föhn, 1973; Stull, 1988; Smeets and others, 1999), although Wieringa (1993) claims it is applicable in moderately anisotropic situations.

### 3. TECHNIQUES

#### 3.1. Field site

Fieldwork was undertaken at Haut Glacier d'Arolla, Valais, Switzerland; a  $\sim 6.3 \text{ km}^2$  valley glacier, with an elevation range of  $\sim 2550$  to  $3500 \text{ m}$  above sea level (a.s.l.), consisting of an upper basin with northwesterly aspect feeding a glacier tongue flowing to the north (Fig. 1). The main field data collection periods were between May and September 1993 and during July and August 1994. Preliminary fieldwork was also conducted in September 1992 and under winter conditions in November 1992 and January and March 1993. The glacier has been the site of several research projects into glacier hydrology, dynamics, meteorology and

**Table 2.** Dates and number of points sampled in 1993 and 1994 glacier surveys

| Glacier survey | Dates                 | N     |      |     |
|----------------|-----------------------|-------|------|-----|
|                |                       | Total | Snow | Ice |
| 1              | 27 & 31 May 1993      | 29    | 29   | 0   |
| 2              | 10 & 11 June 1993     | 34    | 34   | 0   |
| 3              | 26 & 27 June 1993     | 51    | 44   | 7   |
| 4*             | 30 & 31 July 1993     | 56    | 19   | 37  |
| 5              | 17 & 19 August 1993   | 62    | 2    | 60  |
| 6              | 5 to 7 September 1993 | 62    | 36   | 26  |
| 7              | 27 & 28 July 1994     | 36    | 6    | 30  |
| 8              | 18 to 21 August 1994  | 36    | 1    | 35  |

\*Measurements in mid-July 1993 had to be abandoned due to bad weather.

melt in recent years (Richards and others, 1996; Brock and others, 2000; Mair and others, 2002; Strasser and others, 2004). Below about  $3000 \text{ m a.s.l.}$  the surface gradient is shallow (generally  $< 10^\circ$ ), but the upper accumulation area contains steep icefalls, particularly on the north face of Mont Brulé. Most of the glacier's surface can be accessed with relative ease and safety, enabling changing surface conditions to be monitored over large areas.

#### 3.2. Monitoring glacier-wide and seasonal $z_0$ variations

To determine glacier-wide variations in  $z_0$  and related changes in surface conditions, sixty-eight sample points, ranging in elevation from  $2572$  to  $3002 \text{ m a.s.l.}$  were established (Fig. 1). Measurements could not be made safely above  $3000 \text{ m a.s.l.}$  due to steep slopes and crevasses. The western margin of the glacier tongue was not sampled as it is completely moraine-covered. Preliminary fieldwork in 1992 revealed that the spatial variability of  $z_0$  was greatest at low elevations. Accordingly, the spacing of sample points was increased from  $\sim 50 \text{ m}$  on the snout to  $\sim 200 \text{ m}$  in the upper basin. The entire network could be sampled in 2–3 days, producing an almost instantaneous picture of spatial  $z_0$  patterns. The sample point locations were surveyed onto the Swiss Grid using a Geodimeter 400 total station.

The network of points was sampled at 2–3 week intervals throughout the 1993 ablation season (Table 2). The proportion of the sample points monitored increased during the ablation season in response to the increasing variability in surface conditions. Two glacier-wide surveys were also conducted during the 1994 ablation season, at a smaller number of sample points (Table 2), to enable the broad patterns of  $z_0$  variation during 1993 to be compared with those during a second ablation season. Measurements were also made at higher spatial resolution over areas between sample points in 1993, prior to glacier surveys 2 and 4 to assess small-scale  $z_0$  variation. To study the impact of new snowfall and its subsequent melting on  $z_0$ , additional point measurements were made on the days following summer snowfalls on: 21 May, 3 and 13 June and 28 August 1993; and 3 September 1992.

#### 3.3. Microtopographic measurement of $z_0$

Surface microtopography was measured manually using a  $3 \text{ m}$  horizontal reference pole and a metal tape measure. The pole was made out of a hollow plastic tube, rectangular in

cross-section, and marked at 100 mm intervals along its length. At each sample point, surface microtopography was measured by placing the reference pole horizontally on the glacier surface, perpendicular to the prevailing wind direction, and measuring the distance from the base of the reference pole to the glacier surface to the nearest millimetre at horizontal intervals of 100 mm to generate a 3 m profile. The 30 vertical distance measurements generated were substituted into Equation (1) following Munro (1989, 1990) to calculate  $z_0$  for the sample point. This method is quite insensitive to measurement errors. An error of  $\pm 5$  mm at one, several, or all, of the 30 vertical distance measurements made along the reference pole varies  $z_0$  by at most  $\pm 3\%$ , which results in an uncertainty in  $\ln(z_0)$  of  $<1\%$ . Nevertheless, great care was taken to stop the pole from sinking into soft snow surfaces when the pole was supported by only a few points of contact with the surface beneath.

At Haut Glacier d'Arolla, as on most valley glaciers, it was assumed that the prevailing wind was constrained by large-scale topography and flowed either straight up- or down-glacier. Analysis of wind direction data recorded at an automatic weather station located just in front of the glacier snout supports this assumption, with 90% of recorded hourly wind directions in the ablation season within  $\pm 30^\circ$  of two principal modes (up- and down-glacier).

To test whether a 3 m horizontal profile is long enough to generate a representative  $z_0$  value, and whether microtopographic  $z_0$  is independent of the length of the profile used, pairs of  $z_0$  measurements were made at 20 sites using both 3 and 9 m profiles. This comparative sample included fresh snow, three-day old snow, rough snow and ice and debris surfaces. No significant difference was found between  $z_0$  values calculated from 3 and 9 m profiles (t-test,  $p_{H_0} < 0.05$ ). Furthermore, at seven sites 3 m horizontal profile measurements of  $z_0$  were compared with measurements of  $z_0$  using 5, 6, 12 and 15 m profiles. Although some small differences occurred, there was no systematic variation between  $z_0$  generated from 3 m and longer profiles. Based on these data, microtopographic measurement of  $z_0$  is independent of the length of profile, for lengths between 3 and 15 m.

The roughness pole technique was also able to record small-scale microtopography, since vertical height deviations were measured to the nearest millimetre. Thus,  $z_0$  was also measured over very smooth snow surfaces, during the winter and following fresh snowfall.

### 3.4. Explaining $z_0$ variation through surface properties and meteorological variables

An automatic weather station (AWS) was installed  $\sim 200$  m in front of the glacier snout at 2547 m a.s.l., and operated continuously throughout the fieldwork periods, to enable assessment of the effects of meteorological conditions on  $z_0$  and the development of  $z_0$  parameterizations (LMS on Fig. 1). The AWS recorded half-hourly averages of 1 second samples of incoming shortwave radiation ( $W m^{-2}$ ), air temperature ( $^\circ C$ ), relative humidity (%), wind speed ( $m s^{-1}$ ) and direction ( $^\circ$ ) at 2 m height. An identical meteorological station (UMS on Fig. 1) was located on the glacier at 2884 m a.s.l. from 4 July to 25 August 1993 and from 5 July to 23 August 1994. Data from this station were used to determine the local temperature and incoming shortwave radiation lapse rates to extrapolate air temperature and incoming shortwave radiation to all glacier sample points. To determine the relationship between  $z_0$  and accumulated

melt, regular measurements of surface lowering and snow density were made at 16 sample points along the glacier centreline, using ablation stakes. To investigate the relationship of  $z_0$  to snow depth, snow depth was also recorded using a 3 m avalanche probe (error =  $\pm 10$  mm).

### 3.5. Comparison of microtopographic $z_0$ with wind profile $z_0$ measurements

To determine whether the microtopographic measurements generated reliable  $z_0$  values, comparison was made with wind profile  $z_0$  measurements derived from horizontal wind speed and temperature profiles recorded over melting snow and slush, between 9 and 29 July 1994, and over melting ice, between 11 and 24 August 1994 (snow and ice profile sites in Fig. 1). The specific objectives of the comparison were to: (i) determine whether microtopographic  $z_0$  values agreed with profile  $z_0$  values recorded over the same surface and (ii) determine whether microtopographic measurements made in a plane perpendicular, or parallel, to the prevailing wind corresponded with the profile  $z_0$  over an anisotropic surface. Microtopographic measurements were made over the area upwind from the snow profile site (SPS) on 30 occasions between 10 [AUTHOR: should this be 9 as two sentences before?] and 29 July 1994 and on 26 occasions over the area upwind from the ice profile site (IPS) between 11 and 24 August 1994. The upwind area location was determined by the dominant wind direction in the previous 24 hours recorded in the wind profile measurements.

At the SPS and IPS horizontal wind speed and air temperature were measured at 0.5 and 2.0 m above the surface. Samples at 1 Hz were recorded and averaged at 10 minute intervals on a data logger (Campbell Scientific Inc., model CR10, USA). A wind vane (Vector Instruments, model W200P, UK; precision  $6^\circ$ , threshold wind speed  $0.6 m s^{-1}$ ) recorded wind direction at 1.0 m height. Wind speed was measured using pulse output type anemometers (Vector Instruments, model A100M, UK; threshold wind speed  $0.15 m s^{-1}$ , precision  $0.1 m s^{-1}$ ) and air temperature was measured using resistance temperature-curve matched thermistors (precision  $0.4^\circ C$ ) mounted in naturally ventilated radiation shields (Environmental Measurements Ltd, UK). All instruments were mounted on thin aluminium arms (25 mm diameter) supported by a 3 m steel mast (25 mm diameter). A plastic sleeve was drilled into the surface at each site and the base of the mast rested inside the sleeve, supported by a steel screw. Holes were drilled in both the mast and the sleeve at 100 mm intervals, which enabled the mast to be lowered regularly. This, together with adjustments to the heights of the aluminium arms, ensured that the instruments were kept at an approximately constant distance from the glacier surface as it melted.

The 10 minute averaged profile data were assembled into half-hour mean datasets and Monin–Obukhov similarity theory (e.g. Garratt, 1992; Höglstrom, 1988) was used to solve iteratively for friction velocity,  $u^*$ , and temperature scale,  $T^*$ , initially setting bulk stability corrections for momentum,  $\alpha_M$ , and heat,  $\alpha_H$ , to zero:

$$u^* = \frac{k(u_2 - u_1)}{\ln\left(\frac{z_2}{z_1}\right) + \alpha_M\left(\frac{z_2 - z_1}{L}\right)}, \quad (2)$$

$$T^* = \frac{k(T_2 - T_1)}{\text{Pr} \ln\left(\frac{z_2}{z_1}\right) + \alpha_H\left(\frac{z_2 - z_1}{L}\right)}, \quad (3)$$

where  $k$  is von Kármán's constant (0.40) and  $Pr$  is the Prandtl number (0.95). The subscripts 1 and 2, respectively, refer to the lower and upper level measurements of wind speed,  $u$ , and temperature,  $T$ , at height,  $z$ . Then, the first set of  $u^*$  and  $T^*$  values was used to make an initial estimate of the Monin–Obukhov length,  $L$ :

$$L = \frac{u^{*2} \bar{T}}{kgT^*}, \quad (4)$$

in which  $\bar{T}$  is the mean absolute temperature in the surface layer and  $g$  is acceleration due to gravity. The sequence of calculations was repeated, with  $\alpha_M = \alpha_H = 5$ , using each new value from Equation (4), until there was no further change in  $u^*$  and  $T^*$ . A range of stability correction functions exists, but the use of Equation (4) with  $\alpha_M = \alpha_H = 5$  is consistent with the experience that various models give virtually identical results in near-neutral conditions (Andreas, 2002). Near-neutral conditions are here defined for  $0 > z/L < 0.03$ , taking  $z$  to be the height of the upper measurement level. Rearrangement of the log–linear wind profile for use in this range of  $z/L$  yields:

$$u(z) \frac{k}{u^*} = \ln\left(\frac{z}{z_0}\right) + \alpha_M \frac{z}{L}, \quad (5)$$

to generate a  $z_0$  value for each dataset.

In addition to near-neutrality, profile  $z_0$  measurements were only used in the subsequent analyses if the following criteria were met:

1. Height of maximum wind speed  $>2$  m, assumed when  $u_2 > u_1$ .
2. Non-obstructed airflow over fetches of at least 500 m.
3. Natural ventilation of radiation shields with  $u_1 > 3.5 \text{ m s}^{-1}$  ( $>4.5 \text{ m s}^{-1}$  for reflected shortwave radiation  $>50 \text{ W m}^{-2}$ ) to minimize radiative heating effects (Georges and Kasser, 2002). The manufacturer of the radiation shields specifies an error of  $0.4^\circ\text{C}$  for a shortwave radiation flux of  $1000 \text{ W m}^{-2}$  at a wind speed of  $3 \text{ m s}^{-1}$ , hence the temperature measurement error is estimated to be  $\ll 0.4^\circ\text{C}$ .
4. Wind direction range  $<20^\circ$  to allow close identification of the upwind surface cover for comparison with microtopographic measurements.

#### 4. COMPARISON OF MICROTOPOGRAPHIC AND PROFILE $z_0$

Values of the natural logarithm of the aerodynamic roughness length,  $\ln(z_0)$ , are used in this analysis section, since the turbulent fluxes are proportional to the square of  $\ln(z_0)$ . Microtopographic measurements of  $\ln(z_0)$  will be identified as  $\ln(z_{0m})$ , while wind profile measurements will be identified as  $\ln(z_{0p})$ . The use of  $z_0$  will be retained in later sections which describe patterns of  $z_0$  variation, to enable comparison with previously published work, the majority of which also uses  $z_0$ .

##### 4.1. Surface conditions at the snow and ice profile sites (SPS and IPS)

Initially, at the SPS there was a snowpack of  $\sim 1$  m depth marked with surface ablation hollows with vertical relief of  $\sim 0.1$  m and horizontal spacing of  $\sim 0.5$  to  $1.0$  m. The hollows formed a fairly regular pattern with no obvious

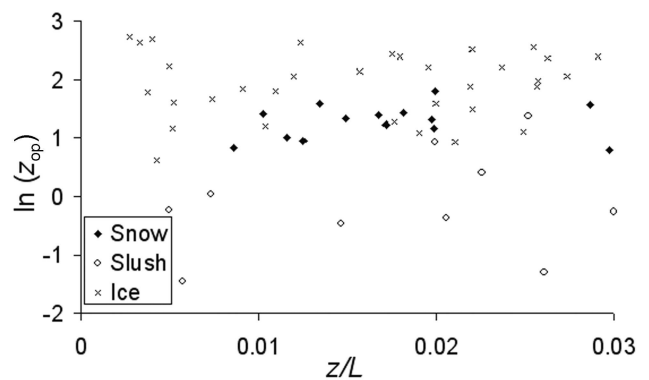


**Fig. 2.** Wind profile derived  $\ln(z_0)$  values plotted against  $z/L$  for snow, slush and ice surfaces. The ranges of wind speed ( $u$ ) and temperature ( $T$ ) corresponding to the  $\ln(z_0p)$  values are: snow,  $u = 4.1\text{--}8.1 \text{ m s}^{-1}$  and  $T = 0.1\text{--}5.1^\circ\text{C}$ ; slush,  $u = 3.5\text{--}5.6 \text{ m s}^{-1}$  and  $T = -0.1\text{--}1.8^\circ\text{C}$ ; ice,  $u = 5.1\text{--}12.1 \text{ m s}^{-1}$  and  $T = -2.1\text{--}3.6^\circ\text{C}$ . The ranges of wind speed and temperature differences between upper and lower measurement levels for each set of  $\ln(z_0p)$  values are as follows: snow,  $u_2 - u_1 = 1.6\text{--}2.2 \text{ m s}^{-1}$ ,  $T_2 - T_1 = 0.3\text{--}1.2^\circ\text{C}$ ; slush,  $u_2 - u_1 = 0.9\text{--}1.6 \text{ m s}^{-1}$ ,  $T_2 - T_1 = 0.1\text{--}0.3^\circ\text{C}$ ; ice,  $u_2 - u_1 = 1.5\text{--}2.9 \text{ m s}^{-1}$ ,  $T_2 - T_1 = 0.1\text{--}1.7^\circ\text{C}$ .

alignment along or across glacier. After 20 July the hollows collapsed as the remaining snowpack turned rapidly to slush, presenting a much smoother surface with vertical dimensions of roughness elements  $\sim 0.01$  m. No measurements were recorded between 20 and 24 July due to a power supply failure. Given the obvious difference in microtopography between the rough snow (before 20 July) and smoother slush surfaces (after 24 July), data for these periods are analysed separately below. Microtopographic measurements were taken perpendicular and parallel-to-wind directions on snow, but only perpendicular-to-wind plane on slush, due to the uniform nature of this surface. The ice surface at the IPS was characterized by foliation bands which formed a series of parallel hummocks and troughs, aligned along glacier, of height  $\sim 0.2$  m and horizontal spacing  $\sim 1.0$  m. Hence, the long axes of the surface roughness elements had strongly preferred orientation aligned with the dominant up- and down-glacier winds. The hummocks continued for over 500 m up- and down-glacier from the IPS, but were interrupted every 10 to 20 m by narrow troughs cutting transverse to the ridges, which probably marked the locations of former crevasses. In contrast to the SPS there was no visible change to the surface microtopography over the measurement period. Apart from a few days of cyclonic weather, conditions were predominantly fine throughout.

##### 4.2. Profile $\ln(z_0)$ values

The  $\ln(z_0p)$  values generated from the profile measurements are plotted against  $z/L$  in Figure 2. On snow and ice the  $\ln(z_0p)$  values are fairly tightly scattered, between 0.79 and 1.81 mm, and 0.63 and 2.73 mm, respectively, but on slush the  $\ln(z_0p)$  values display larger scatter between  $-1.45$  and  $1.38$  mm. None of the  $\ln(z_0p)$  results show any trend across the stability range.

**Table 3.** Comparison of wind profile and microtopographic  $\ln(z_0)$  over rough snow, slush and ice surfaces at the snow and ice profile sites;  $\sigma$  — standard deviation of the sample

| Surface type | Method                             | Sample size | $\ln(z_0)$               | $z_0$      |
|--------------|------------------------------------|-------------|--------------------------|------------|
|              |                                    |             | Mean $\pm 1\sigma$<br>mm | Mean<br>mm |
| Snow         | Wind profile                       | 14          | $1.27 \pm 0.30$          | 3.56       |
|              | Microtopographic:<br>perpendicular | 24          | $0.84 \pm 0.56$          | 2.31       |
|              | Microtopographic:<br>parallel      | 24          | $0.48 \pm 0.76$          | 1.62       |
| Slush        | Wind profile                       | 10          | $-0.13 \pm 0.88$         | 0.88       |
|              | Microtopographic:<br>perpendicular | 6           | $-0.42 \pm 0.35$         | 0.65       |
| Ice          | Wind profile                       | 34          | $1.93 \pm 0.57$          | 6.89       |
|              | Microtopographic:<br>perpendicular | 14          | $1.94 \pm 0.32$          | 6.96       |
|              | Microtopographic:<br>parallel      | 12          | $-0.13 \pm 1.09$         | 0.88       |

### 4.3. Comparison of microtopographic and wind profile $\ln(z_0)$ on snow

The mean  $\ln(z_{0m})$  values from perpendicular ( $\ln(z_{0m}) = 0.84$  mm) and parallel ( $\ln(z_{0m}) = 0.48$  mm) microtopographic profiles are slightly lower than the mean  $\ln(z_{0p})$  value of 1.27 mm, but there is a large overlap in the ranges (mean  $\pm 1$  standard deviation of the mean) of  $\ln(z_{0m})$  and  $\ln(z_{0p})$  (Table 3). The upper end of the  $\ln(z_{0p})$  and  $\ln(z_{0m})$  ranges are similar, whereas the bottom end of the  $\ln(z_{0m})$  range is much smaller than the lowest  $\ln(z_{0p})$  value. Statistically, there is no significant difference between  $\ln(z_{0m})$  in perpendicular and parallel profiles ( $t$ -test,  $pH_0 < 0.05$  [AUTHOR: I am unfamiliar with  $pH_0$ , so am not sure I have italicised it correctly. I have assumed the 'p' indicates probability, so should be upright and 'H<sub>0</sub>' is a variable, so the 'H' should be italic. OK?]), as expected from the homogenous nature of the snow surface. Visually, the mean perpendicular  $\ln(z_{0m})$  value corresponds most closely with the mean  $\ln(z_{0p})$  value.

### 4.4. Comparison of microtopographic and wind profile $\ln(z_0)$ on slush

The mean  $\ln(z_{0p})$  value of  $-0.13$  mm on slush is significantly lower than the corresponding value on the rough snow surface ( $t$ -test,  $pH_0 < 0.001$ ; Table 3). The mean  $\ln(z_{0m})$  value of  $-0.42$  mm corresponds closely with the mean  $\ln(z_{0p})$  and the  $\ln(z_{0m})$  range is completely within the  $\ln(z_{0p})$  range (Table 3).

### 4.5. Comparison of microtopographic and aerodynamic $\ln(z_0)$ on ice

The mean  $\ln(z_{0m})$  value from perpendicular microtopographic profiles of 1.94 mm is almost exactly equal to the mean  $\ln(z_{0p})$  value of 1.93 mm, and the  $\ln(z_{0m})$  range for perpendicular profiles is entirely within the  $\ln(z_{0p})$  range (Table 3). In contrast, the mean  $\ln(z_{0m})$  value of  $-0.13$  mm from parallel microtopographic profiles is significantly lower than the equivalent  $\ln(z_{0p})$  and perpendicular microtopographic profile  $\ln(z_{0m})$  values ( $t$ -test,  $pH_0 < 0.0001$ ; Table 3).

**Table 4.** Variation in mean  $\ln(z_{0p})$  ( $10^{-3}$  m) and mean  $z_{0p}$  ( $10^{-3}$  m) with adjustment to instrument base height level for snow, slush and ice surface types

| Surface type |              | Height adjustment |           |          |
|--------------|--------------|-------------------|-----------|----------|
|              |              | $-50$ mm          | $0$ mm    | $+50$ mm |
| Snow         | $\ln z_{0p}$ | 0.75              | 1.27      | 1.72     |
|              | $z_{0p}$     | 2.11              | 3.56      | 5.58     |
| Slush        | $\ln z_{0p}$ | $-0.82$           | $-0.13$   | 0.45     |
|              | $z_{0p}$     | 0.44              | $0.88z_0$ | 1.57     |
| Ice          | $\ln z_{0p}$ | 1.61              | 1.93      | 2.23     |
|              | $z_{0p}$     | 5.00              | 6.89      | 9.30     |

### 4.6. Comparison of microtopographic and aerodynamic $\ln(z_0)$ : discussion

The results support the application of the microtopographic method to measurement of  $\ln(z_0)$  over melting glacier surfaces. While the range of mean  $\ln(z_0)$  values in the study was not very large, it spans the 0.1 to 1.0 mm  $z_0$  scale, and surface types, typical of glacier surfaces during the ablation season (Table 1). The  $\ln(z_{0p})$  values (and perpendicular  $\ln(z_{0m})$  values) are significantly different between the rough snow, slush and ice surfaces ( $t$ -test,  $pH_0 < 0.001$ ), indicating that these are distinct surface types with their own characteristic aerodynamic roughness length values. The  $\ln(z_{0m})$  values generated from profiles made perpendicular to the prevailing wind are statistically the same as the  $\ln(z_{0p})$  values recorded over the same surface type ( $t$ -tests,  $pH_0 < 0.01$ ; Table 3). However,  $\ln(z_{0m})$  values recorded from profiles parallel to the prevailing wind were significantly lower than  $\ln(z_{0p})$  on the anisotropic ice surface ( $t$ -test,  $pH_0 < 0.0001$ ; Table 3), but similar to  $\ln(z_{0p})$  on the more isotropic snow surface. This implies that, where roughness elements have a strong orientation, microtopographical measurements made in a wind-parallel plane do not effectively record the upwind face areas of the surface roughness elements; typically the areas are underestimated. No glacier surfaces were encountered where the long axis of roughness elements was aligned across glacier. It cannot therefore be determined whether parallel or perpendicular microtopographic measurements would correspond to  $\ln(z_{0p})$  where microtopography is rougher in the parallel-to-wind direction than in the perpendicular-to-wind direction. Such a configuration of roughness elements is not likely to be common on mountain glaciers, however, since ice dynamics and the action of meltwater tend to generate ridges and troughs aligned along glacier (Goodsell and others, 2003). Hence, microtopographic  $\ln(z_0)$  measurements should be made using roughness pole profiles aligned perpendicular to the prevailing wind, as defined in section 3, particularly where roughness elements do not form a homogenous pattern.

The results suggest that accurate (by comparison to vertical wind profile measurements)  $\ln(z_0)$  values can be obtained from samples of about six microtopographic measurements. On both slush and ice surfaces, the  $\ln(z_{0m})$  range was smaller than that of  $\ln(z_{0p})$  (Table 3). On both of these surfaces there was little spatial variation in the vertical dimensions of surface roughness elements. In contrast, on rough snow the range of  $\ln(z_{0m})$  was larger than that for



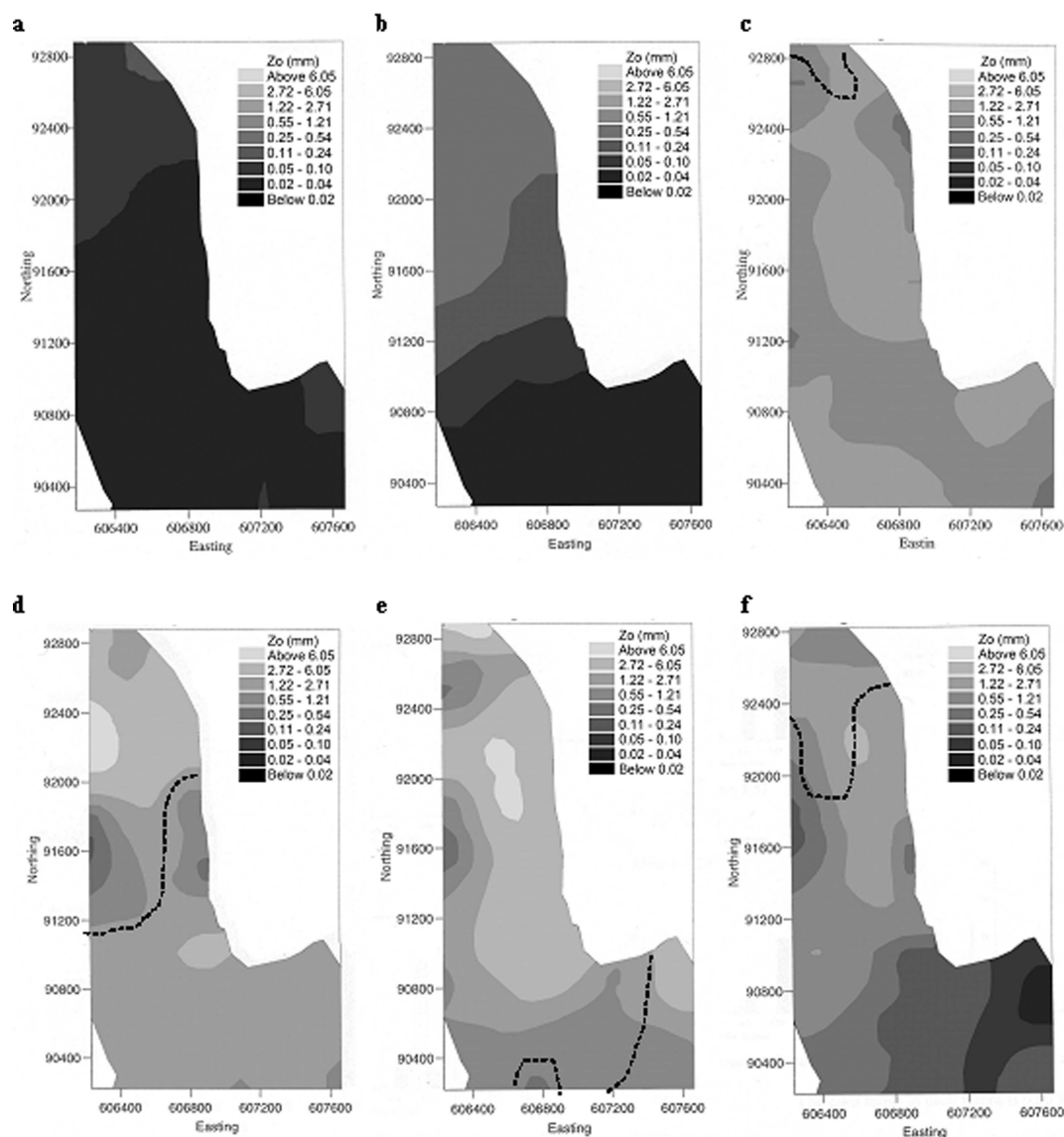


**Fig. 3.** Maps of  $z_0$  variation across sampled areas of Haut Glacier d'Arolla in (a) late May, (b) early June, (c) late June, (d) late July, (e) mid-August and (f) early September 1993. The dashed line marks the approximate position of the transient snowline;  $z_0$  class sizes are equal divisions of  $0.80 \ln(z_0)$ . A standard 'fault' interpolation routine was used, which did not alter the original  $z_0$  values (UNIRAS, 1990). Eastings and Northings are on the Swiss National Grid in metres.

$\ln(z_{0p})$  (Table 3). On this surface there was some spatial variation in the vertical extent of roughness elements, i.e. ablation hollows developed to varying sizes over different areas upwind from the SPS. It appears that the larger element sizes controlled  $\ln(z_0)$  on this surface given the close correspondence between the upper range of  $\ln(z_{0m})$  and the mean  $\ln(z_{0p})$  (Table 3).

Incorrect identification of the base level for the instrument heights is a possible error source in the  $\ln(z_{0p})$  measurements. Munro (1989) added 0.17 m (the typical vertical extent of the surface roughness elements) to instrument heights in the calculation of  $\ln(z_{0p})$  at Peyto Glacier, Canada, while Andreas (2002), in a reanalysis of the same dataset, deemed such a height adjustment to be unnecessary. Doubt over the instrument heights adds uncertainty to  $\ln(z_{0p})$  values. An adjustment to instrument heights of  $\pm 50$  mm leads to a large change in the mean  $\ln(z_{0p})$  value (Table 4). The height uncertainty is not great enough, however, to explain the large decrease in  $\ln(z_{0p})$

between rough snow and slush at the SPS. Reduction of the instrument heights by 0.1 m (the typical vertical extent of roughness elements) over rough snow, reduces the mean  $\ln(z_{0p})$  to 0.41 mm which is still much larger than the mean  $\ln(z_{0p})$  recorded over slush.

## 5. DESCRIPTION OF $z_0$ VARIATIONS ACROSS HAUT GLACIER D'AROLLA

In this section the patterns of  $z_0$  variation across Haut Glacier d'Arolla during the 1993 and 1994 ablation seasons are described, based on the microtopographic measurements made during the eight glacier surveys (Table 2). Values of  $z_0$  (mm) are used to enable comparison with previous published work.

The sample point microtopographic measurements were interpolated to display the  $z_0$  variation across the sampled area of the glacier during each completed 1993 glacier survey (Fig. 3a–f). Diagrams displaying the frequency

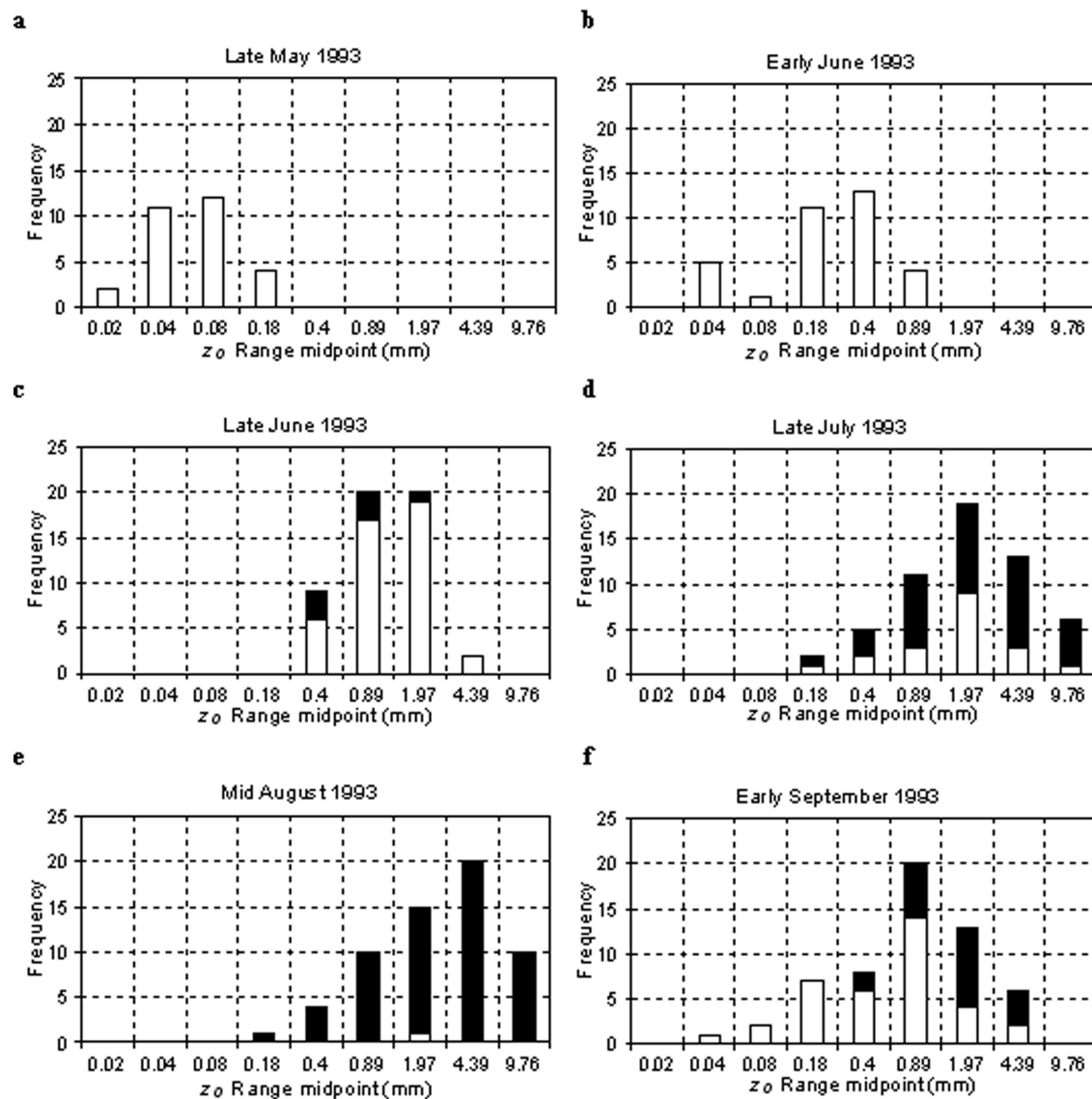
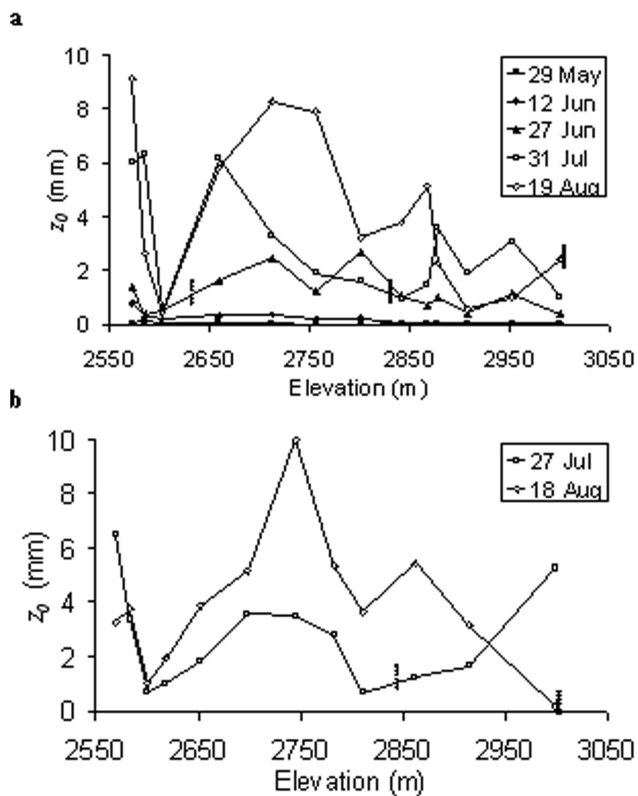


Fig. 4. Frequency distributions of sample point  $z_0$  during each glacier survey in 1993. Black – ice, white – snow. (Bin size –  $0.80 \ln(z_0)$ .)

distributions of sample point  $z_0$  during each 1993 survey and spatial  $z_0$  variation along the glacier centreline are shown in Figures 4 and 5, respectively. The main glacier-wide patterns of  $z_0$  variation which emerge are as follows:

1. Low spatial  $z_0$  variation at the start of the ablation season (Fig. 3a) changed to high spatial variation, particularly during the mid- (Fig. 3d–e), and late (Fig. 3f) ablation season. Correspondingly, the  $z_0$  range was small during May and June (Fig. 4a–c), but large during July, August and September (Fig. 4d–f). This reflects the transition from a complete glacier-wide smooth snow cover in late May, to a variety of surface types, e.g. snow ablation hollows, slush, smooth and rough areas of ice and debris cover.
2. The dominant spatial  $z_0$  patterns were: (i)  $z_0$  varied independently of elevation, except during early June (Fig. 3b) and in the upper basin during early September (Fig. 3f); (ii) with the exception of late May and early June (Fig. 3a,b),  $z_0$  varied across glacier, particularly over the tongue during July, August and September (Fig. 3d–f), when  $z_0$  was highest in the middle and lowest at the margins, particularly along the western margin; (iii) between late June and August, snow and ice had very similar  $z_0$  values (Fig. 4c–e). Consequently the snowline was not associated with clear change in  $z_0$  at any stage of the ablation season (Fig. 3a–f).
3. The main temporal trends were: (i) snow  $z_0$  increased from  $\leq 0.10$  mm in late May [AUTHOR: Should this be **0.18** rather than **0.1**, as fig 4?] to between  $\sim 0.5$  and 10 mm from late June to August (Figs 3a–f and 4a–f); (ii)  $z_0$  decreased, to values as low as  $< 0.10$  mm following fresh snowfalls, e.g. in the upper basin between August and September 1993 (Figs 3e,f and 4e,f). Following snowfall,  $z_0$  initially remained low for 1–2 days, but as the fresh snow melted over the next few days there was a rapid increase in the underlying ice or snow  $z_0$  value; (iv) ice  $z_0$  increased between late June and August at many points, especially over the centre of the glacier tongue (Figs 3c–e and 5a). However, it decreased at other points, e.g. over the northwestern part of the glacier tongue between late July and August 1993 (Fig. 3d,e) and over the lower tongue between August and September



**Fig. 5.** Variation of  $z_0$  along the centreline long profile during the (a) 1993 and (b) 1994 ablation seasons. The dashed line marks the approximate position of the snowline on each profile.

1993 (Fig. 3e,f). Areas of relatively rough ice, e.g. at 2700–2750 m a.s.l., and relatively smooth ice, e.g. at 2600 m a.s.l., persisted throughout both the 1993 and 1994 ablation seasons (Fig. 5a,b).

- Spatial variation of  $z_0$  was generally small on the ablating winter snowpack, both when the surface was smooth or characterized by ‘ablation hollows’ (Fig. 3a–d). However, spatial variation of ice  $z_0$  was more complex (Figs 3d,e and 5a,b). Particularly noticeable was an area of smooth ice ( $z_0 < 1$  mm) at  $\sim 2600$  m elevation, which contrasted markedly with the debris-covered ice down-glacier and rough ice up-glacier (Figs 3e and 5a,b). A snowstorm on 4 September 1993 covered areas above 2650 m a.s.l. with fresh snow ranging from a thin and patchy cover on the lower tongue to a continuous blanket, with mean depth of  $\sim 100$  mm in the upper basin. The spatial pattern of ice  $z_0$  variation recorded in August could be ‘seen’ through the fresh snow cover over most of the glacier tongue, but on the upper tongue and basin the snow cover was deep enough to smooth the ice roughness elements (Fig. 3e, f).

## 6. PARAMETERIZATION OF $z_0$ VARIATIONS

In this section parameterizations of  $\ln(z_0)$  variations, based on independent variables which may be used in numerical melt models, are developed. Parameterizations are developed first for snow, followed by ice and finally for fresh snowfalls on ice.

**Table 5.** Correlations of dependent variables: snow  $\ln(z_0)$  ( $\ln(z_{0S})$ ); ice  $\ln(z_0)$  ( $\ln(z_{0I})$ ) and  $\ln(z_0)$  following snowfall on an ice surface ( $\ln(z_{0SI})$ ) with independent variables: accumulated melt ( $M_a$ ); accumulated daily maximum temperatures ( $T_a$ ); accumulated daily mean incoming shortwave radiation ( $R_a$ ); accumulated days ( $D_a$ ); snow depth ( $d$ ) and underlying ice  $\ln(z_0)$  ( $\ln(z_{0I})$ ). See text for full definition of variables. Correlations significant at the 0.05 level are shown in bold. The degrees of freedom for each correlation are given in brackets. A dash indicates insufficient data to attempt a correlation

|                | $\ln(z_{0S})$       | $\ln(z_{0I})$      | $\ln(z_{0SI})$     |
|----------------|---------------------|--------------------|--------------------|
| $\log_{10}M_a$ | <b>0.886 (48)</b>   | 0.040 (82)         | –                  |
| $\log_{10}T_a$ | <b>0.811 (177)</b>  | <b>0.234 (239)</b> | <b>0.337 (63)</b>  |
| $\log_{10}R_a$ | <b>0.779 (189)</b>  | –                  | –0.027 (63)        |
| $\log_{10}D_a$ | <b>0.805 (189)</b>  | 0.097 (239)        | 0.072 (63)         |
| $d$            | <b>–0.523 (147)</b> | –                  | <b>–0.274 (63)</b> |
| $\ln(z_{0I})$  | –                   | –                  | <b>0.533 (63)</b>  |

### 6.1. Snow $\ln(z_0)$ : $\ln(z_{0S})$

The independent variables: accumulated melt ( $M_a$ ; millimetre water equivalent (mm w.e.)), accumulated daily maximum temperature ( $T_a$ ; °C), accumulated daily mean incoming shortwave radiation ( $R_a$ ;  $\text{W m}^{-2}$ ) and accumulated days ( $D_a$ ), each of which increases from a value of zero at the time of the most recent snowfall, and snow depth ( $d$ ; m) were used to explain  $\ln(z_{0S})$  variations. These variables may account for the increasing roughness of snow surfaces with time through the formation of ablation hollows associated with local melt rate variations (Hunt, 1993). The variables  $M_a$ ,  $T_a$  and  $d$  might also explain spatial patterns of  $\ln(z_{0S})$  through their correlations with the up-glacier decrease in the surface melt rate. There was no significant variation in shortwave radiation receipts between the LMS and UMS and it was therefore assumed that incoming shortwave radiation was uniform across the glacier. Based on the mean difference in temperatures between the UMS and LMS a uniform lapse rate of  $0.9^\circ\text{C}$  per 100 m rise in elevation was applied to the temperature data.

All independent variables are correlated significantly with  $\ln(z_{0S})$  and the strongest correlations are those for the four accumulated independent variables (Table 5). However, the relationships between  $\ln(z_{0S})$  and accumulated variables are non-linear, being characterized by three distinct phases in each case (Fig. 6a–d). At both low and high values of the accumulated independent variables,  $\ln(z_{0S})$  varies little (for  $\ln(z_{0S})$  values between about  $-5$  to  $-2.5$  mm and about  $-0.5$  to  $2$  mm, respectively), but these phases are separated by a period of rapid increase in  $\ln(z_{0S})$  at medium values of each accumulated independent variable. These graphs suggest that the formation of ablation hollows in a melting snow surface begins slowly, but once hollows have initiated their growth proceeds rapidly, until some self-limiting condition is reached. This might occur when shading of the bottom of the hollows, or concentration of impurities in the snow act to halt their growth (Hunt, 1993). It can also be seen that  $\ln(z_{0S})$  increases with decreasing snow depth, although there is large scatter in this relationship (Fig. 6e). At snow depths less than  $\sim 0.7$  m, there are no  $\ln(z_{0S})$  values lower than  $-2.0$  mm ( $z_{0S} = 0.14$  mm), probably due to a combination of well-developed ablation hollows on old snow surfaces and the

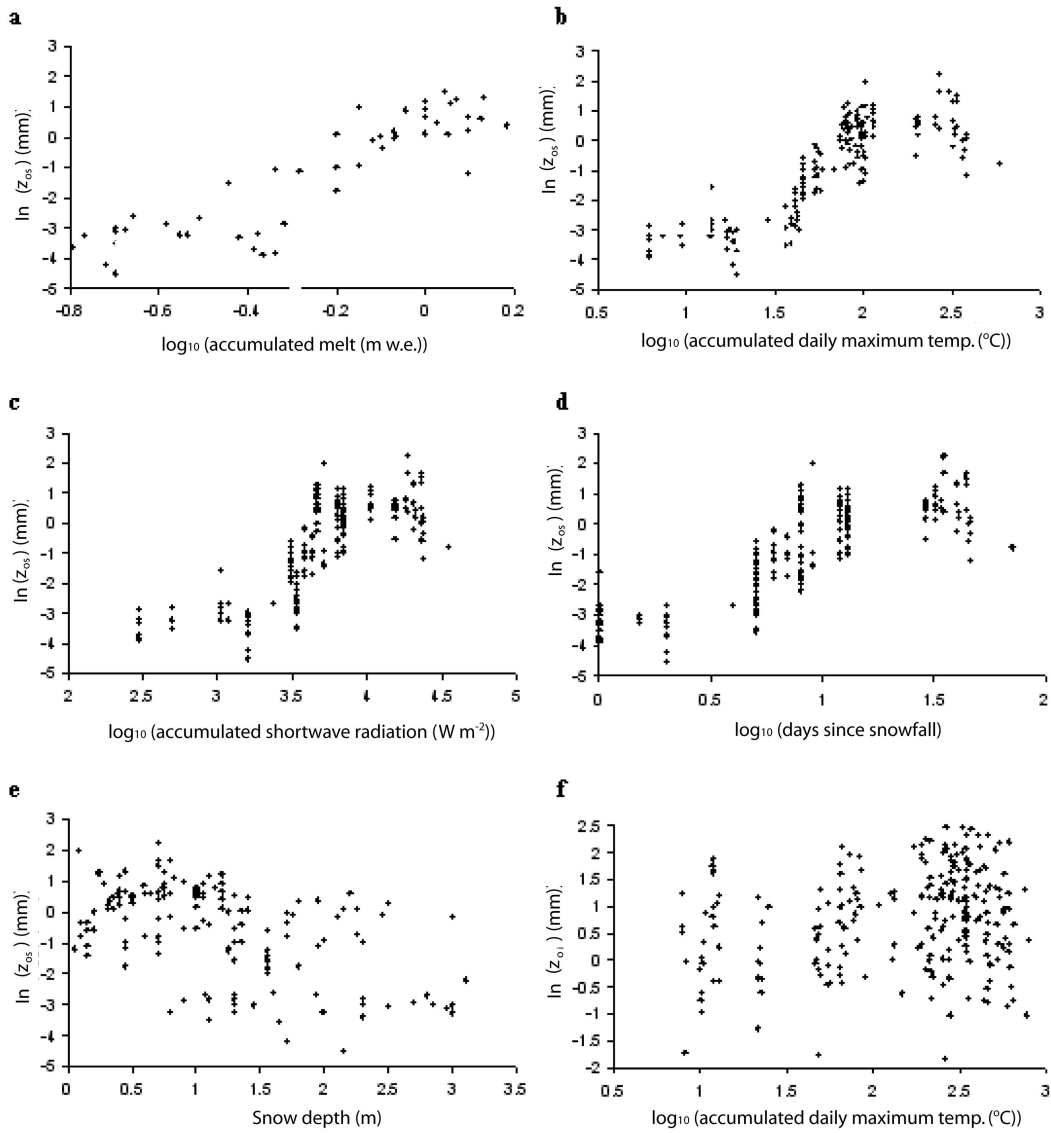


**Fig. 6.** Relationships between snow  $\ln(z_{0s})$  and (a) accumulated melt, (b) accumulated daily maximum temperature, (c) accumulated daily mean incoming shortwave radiation, (d) accumulated days and (e) snow depth. (f) Relationship between ice  $\ln(z_{0i})$  and accumulated daily maximum temperature.

influence of the underlying ice microtopography on fresh shallow snow covers.

Two forms of parameterization were applied. First a linear equation of the form:

$$\ln(z_0) = a + b_1 V_1 + b_2 V_2 + \dots, \quad (6)$$

in which  $a$  and  $b_x$  are coefficients and  $V_x$  are independent variables. Second, a non-linear equation was applied to explain the stepped form of the relationship between  $\ln(z_{0s})$  and the accumulated independent variables:

$$\ln(z_0) = b_1 \{ \text{atan}[(V + b_2)/b_3] \} + b_4, \quad (7)$$

**[AUTHOR: I have assumed 'a' is not a coefficient. OK? (should it be arctan?) do you think your readers may be confused?]** in which  $b_x$  are coefficients and  $V$  is an independent variable. A stepwise regression procedure was used to identify the relationships that explain the largest amount of  $\ln(z_{0s})$  variation using any combination of the independent variables (Table 6).

The stepped form of the relationships of  $\ln(z_{0s})$  to  $M_a$ ,  $T_a$ ,  $R_a$  and  $D_a$  is better represented by the non-linear regressions

(Equation (7)) than by the linear regressions (Equation (6)). The non-linear parameterization based on  $M_a$  explains the largest amount of  $\ln(z_{0s})$  variation, as indicated by its  $R^2$  value but, since the parameterizations based on  $T_a$ ,  $R_a$  and  $D_a$  are calibrated with much larger datasets, these relationships are probably better parameterizations of  $\ln(z_{0s})$  variation (Table 6). Furthermore, a  $\ln(z_{0s})$  parameterization based on  $M_a$  may introduce a circularity problem in a melt model, since the melt rate, i.e. the output from the melt model, must be known a priori. Errors in the initial  $\ln(z_{0s})$  value will generate errors in the melt rate which, in turn, might lead to greater error in  $\ln(z_{0s})$ , and thus amplify over time. Overall, the most successful parameterization for  $\ln(z_{0s})$  is the non-linear equation based on  $T_a$  (Fig. 7):

$$\ln(z_{0s}) = 1.34 \{ \text{atan}[(T_a - 1.68)/0.10] \} - 1.40. \quad (8)$$

The non-linear parameterizations using  $R_a$  and  $D_a$  offer good alternatives depending on data availability and the modelling approach used. For parameterizations using  $T_a$  (Equation (8)) under the condition  $T_a < 0$ , the minimum asymptotic value of  $\ln(z_{0s})$  of  $-3.5$  mm ( $z_{0s} = 0.03$  mm)

should be applied, as negative number logarithms cannot be found.

### 6.2. Ice $\ln(z_0)$ : $\ln(z_{0i})$

The independent variables:  $M_a$ ,  $T_a$ ,  $D_a$ , each of which increases from a value of zero at the time the ice surface is first exposed following melting of the overlying snow cover, and elevation,  $E$ , were used to explain  $\ln(z_{0i})$  variations. The accumulated variables are included as surface roughness may increase over time due to small-scale melt rate differentials. All measurements made over ice surfaces were initially included in the analyses. Subsequently, the dataset was divided between: (i) initial  $\ln(z_{0i})$  values recorded at each point immediately following melting of the overlying snow cover, in order to examine  $\ln(z_{0i})$  as a function of  $E$  alone and (ii) the change in  $\ln(z_{0i})$  from its initial  $\ln(z_{0i})$  value over time,  $\Delta\ln(z_{0i})$ , in order to examine temporal  $\ln(z_{0i})$  trends alone.

The relationships between  $\ln(z_{0i})$  and the independent variables are weak; only the positive correlation with  $T_a$  is significant (Table 5, Fig. 6f). The initial  $\ln(z_{0i})$  values are not significantly correlated with elevation and  $\Delta\ln(z_{0i})$  is not significantly correlated with any independent variable at the 0.05 significance level. Figure 6f shows little evidence for the pattern of increasing  $\ln(z_{0i})$  between June and August, followed by decreasing  $\ln(z_{0i})$  towards the end of the ablation season, which was suggested by Figure 3c–e. Instead,  $\ln(z_{0i})$  both increased and decreased over time on different parts of the glacier following melting of the overlying snow cover, with no general trends apparent.

An attempt to parameterize  $\ln(z_{0i})$  as a function of  $T_a$  was unsuccessful as this variable explained an insignificant amount of  $\ln(z_{0i})$  variation. One approach to  $\ln(z_{0i})$  parameterization in a numerical model is to use the mean  $\ln(z_{0i})$ . The mean  $\ln(z_{0i})$  at Haut Glacier d'Arolla is 0.81 mm ( $z_{0i} = 2.24$  mm). The standard deviation of  $\ln(z_{0i})$  of 0.89 mm gives a range of  $\ln(z_{0i})$  of 0.08 to 1.7 mm ( $z_{0i}$  range: 0.92 to 5.47 mm). Although errors in calculating spatial and temporal variations in turbulent fluxes will arise from using a constant mean  $\ln(z_{0i})$  value, these errors will

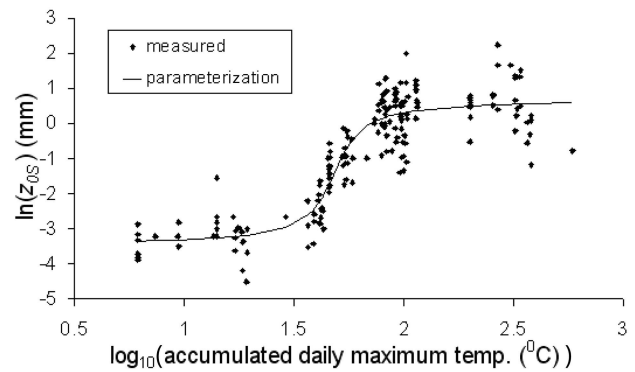


**Fig. 7.** Variation of the non-linear  $\ln(z_{0s})$  parameterization (Equation (8)) and measured  $\ln(z_{0s})$  values, with accumulated daily maximum temperatures since snowfall.

tend to cancel when making calculations over the ablation season for an entire glacier. An alternative is to sample  $\ln(z_{0i})$  randomly from a frequency distribution defined by the mean and standard deviation of  $\ln(z_{0i})$ , in order to better simulate the likely range of turbulent flux values over ice (Brock and others, 2000).

### 6.3. The $\ln(z_0)$ following fresh snowfall on an ice surface: $\ln(z_{0Si})$

When fresh snow falls on a rough ice surface,  $\ln(z_{0Si})$  is strongly influenced by the underlying roughness elements if the fresh snow is too shallow to blanket the underlying ice roughness elements. Following snowfalls on ice surfaces  $\ln(z_{0Si})$  was most strongly correlated with the underlying ice  $\ln(z_0)$  (Table 5), demonstrating the important influence of the underlying ice topography on the surface roughness of shallow snow covers. There is a tendency for  $\ln(z_{0Si})$  to increase following snowfall, as the fresh snow melts and more of the underlying roughness elements are exposed, as demonstrated by the negative correlation with  $d$  and the positive correlation with  $T_a$  (Table 5). The tendency for

**Table 6.** Parameterizations of  $\ln(z_0)$ : coefficient values and summary statistics;  $R^2$  is the coefficient of determination. The standard error is given in brackets after each coefficient value

| Dependent variable        | Independent variable  | Coefficient values |              |              |              | $R^2$ | $pH_0$  | $N$ |
|---------------------------|-----------------------|--------------------|--------------|--------------|--------------|-------|---------|-----|
|                           |                       |                    |              |              |              | %     |         |     |
| Linear (Equation (6))     |                       |                    |              |              |              |       |         |     |
|                           |                       | $a$                | $b_1$        | $b_2$        | $b_3$        |       |         |     |
| $\ln(z_{0s})$             | $M_a$                 | 0.20 (0.17)        | 5.55 (0.45)  | –            | –            | 78.0  | <0.0001 | 50  |
| $\ln(z_{0s})$             | $T_a$                 | 6.19 (0.30)        | 2.96 (0.16)  | –            | –            | 65.6  | <0.0001 | 179 |
| $\ln(z_{0s})$             | $R_a$                 | –11.10 (0.63)      | 2.81 (0.17)  | –            | –            | 60.5  | <0.0001 | 177 |
| $\ln(z_{0s})$             | $D_a$                 | –3.36 (0.15)       | 2.74 (0.15)  | –            | –            | 64.6  | <0.0001 | 191 |
| $\ln(z_{0Si})$            | $\ln(z_{0i}), T_a, d$ | –1.69 (0.32)       | 0.60 (0.13)  | 1.03 (0.27)  | –5.38 (2.14) | 45.5  | <0.0001 | 64  |
| $\ln(z_{0Si})$            | $T_a, d$              | –1.09 (0.35)       | 0.92 (0.30)  | –6.66 (2.53) | –            | 18.6  | <0.002  | 64  |
| Non-linear (Equation (7)) |                       |                    |              |              |              |       |         |     |
|                           |                       | $b_1$              | $b_2$        | $b_3$        | $b_4$        |       |         |     |
| $\ln(z_{0s})$             | $M_a$                 | 1.46 (0.18)        | 0.23 (0.03)  | 0.08 (0.04)  | –1.30 (0.14) | 85.8  | <0.0001 | 50  |
| $\ln(z_{0s})$             | $T_a$                 | 1.34 (0.07)        | –1.68 (0.01) | 0.10 (0.02)  | –1.40 (0.07) | 83.1  | <0.0001 | 179 |
| $\ln(z_{0s})$             | $R_a$                 | 1.22 (0.07)        | –3.56 (0.01) | 0.07 (0.02)  | –1.32 (0.08) | 77.8  | <0.0001 | 177 |
| $\ln(z_{0s})$             | $D_a$                 | 1.38 (0.09)        | –0.77 (0.02) | 0.15 (0.03)  | –1.41 (0.09) | 75.0  | <0.0001 | 191 |

summer snowfalls to be followed by clear days with sub-zero temperatures and little or no surface melt could explain why  $\ln(z_{0SI})$  is not correlated with  $R_a$  or  $D_a$  (Table 5).

It is possible to parameterize  $\ln(z_{0SI})$  through a multiple regression relationship (Equation (6)) on the independent variables underlying  $\ln(z_{0SI})$ ,  $T_a$  and  $d$ , which explains >45% of the variation in  $\ln(z_{0SI})$  (Table 6). If the underlying  $\ln(z_{0SI})$  is not known,  $\ln(z_{0SI})$  can be parameterized using  $T_a$  and  $d$  alone (Table 6). Hence, the  $\ln(z_{0SI})$  of fresh snowfalls on rough underlying ice surfaces can be parameterized separately from 'deep' snowpacks (section 6.1) in a numerical melt model.

## 7. DISCUSSION AND CONCLUSIONS

As far as the authors are aware, this study is the first attempt to systematically monitor and parameterize changes in aerodynamic roughness length over a valley glacier throughout the ablation season, and to validate microtopographic  $z_0$  measurements with independent vertical wind profile estimates of  $z_0$  over snow, slush and ice surfaces. The main findings are as follows.

### 7.1. Validity of the microtopographic $z_0$ measurement technique

The close agreement of microtopographic  $z_0$  measurements with independent wind profile  $z_0$  measurements over snow, slush and ice surfaces (section 4), provides strong support for the use of microtopographic  $z_0$  measurements of over melting glacier surfaces. Indeed, the microtopographic measurements had lower scatter than the profile measurements over slush and ice, despite the careful selection criteria applied to obtain reliable wind profile  $z_0$  estimates. The microtopographic technique may well be the better of the two techniques over melting glacier surfaces, if the uncertainty of the base level for instrument heights is considered in wind profile  $z_0$  calculations. Further validation of the microtopographic technique is needed, however, in particular over surfaces where roughness element size is spatially variable. Our results suggest that  $z_0$  is controlled by the larger-sized elements over such surfaces.

The wind profile  $z_0$  measurements relied on only two measurement levels and naturally ventilated temperature shields, which represents the minimum instrumentation necessary for this technique, creating difficulty in determining the instruments' base height. The strict data selection criteria applied, in particular, the requirement of high wind speeds and near-neutral atmospheric conditions, together with careful monitoring of instrument heights throughout the experiments ensure that the resulting profile  $z_0$  values are reliable; a conclusion which is corroborated by the close similarity of our profile  $z_0$  values with  $z_0$  values reported over similar surface types in other studies using more detailed profiles or eddy covariance measurements. Recent improvements to micrometeorological instrumentation deployable on glaciers should facilitate more reliable comparisons between the wind profile and microtopographic techniques in the future.

The validation of the microtopographic technique was limited to fairly rough surfaces with roughness elements at the centimetre to decimetre scale ( $z_0$  at the 0.1–1 mm scale), but we demonstrate the microtopographic technique is also applicable to smoother surfaces in the  $z_0 = 0.01$ –0.1 mm range. In order to obtain reliable microtopographic measure-

ments, a 3 m pole is sufficient for surfaces where  $z_0 \leq 10$  mm. If a shorter pole is used it is unlikely that a sufficient sample of surface roughness elements will be recorded, while for surfaces where the vertical dimensions of the elements are >1 m, a longer pole should be used. Microtopographic measurements should be made with the pole aligned perpendicular to the prevailing wind direction, particularly where roughness elements' long axes have a preferred orientation. If the pole is aligned parallel to the wind, the upwind face area of elements may be underestimated, leading to an underestimate of  $z_0$ . The conversion of height deviations recorded in a microtopographic profile to  $z_0$ , following the method of Munro (1989), is based on a simplification of element forms into regular cube shapes. This is a necessary generalization given that the original formula of Lettau (1969) was developed by placing bushel baskets on a frozen lake, and due to the difficulty of measuring and converting irregularly shaped elements into a  $z_0$  value.

The microtopographic method has a distinct advantage over other  $z_0$  measurement methods in that it enables repeated measurements to be made at many points across a glacier surface. Given the large spatial and temporal variations in  $z_0$  recorded across Haut Glacier d'Arolla during two ablation seasons, such a sampling strategy is essential to generate representative  $z_0$  values for the modelling of turbulent fluxes and surface melt rate variations.

### 7.2. Seasonal patterns of $z_0$ variation: description and parameterization for numerical melt models

Values of  $z_0$  in the range 0.01 to 0.10 mm, recorded at Haut Glacier d'Arolla over fresh snow and during the winter, are lower than those previously reported for valley glaciers, but similar to those recorded over Antarctic snow surfaces (Table 1b). On older melting snow our  $z_0$  values of 0.1 to 5 mm are similar to those reported for other mountain glaciers. For ice, the  $z_0$  values at Haut Glacier d'Arolla are similar to old melting snow surfaces, but slightly larger (mean = 2.24 mm) with a higher upper limit of ~10 mm. The ice  $z_0$  values at Haut Glacier d'Arolla are similar to those reported for other glaciers, although well below the extremes reported by Duynkerke and Van den Broeke (1994), Smeets and others (1999) and Obleitner (2000) (Table 1). **[AUTHOR: I am not sure where the mean values and ranges given for this work in this paragraph are shown. Would it help the readers to refer to a fig or table?]**

Snow  $z_0$  exhibited the same clear trend during the both 1993 and 1994 ablation seasons at Haut Glacier d'Arolla. Initially,  $z_0$  increased very gradually from sub-millimetre values early in the ablation season or following fresh snowfall, then underwent a period of rapid increase over a few weeks before stabilizing at values of a few millimetres in the mid- to late ablation season. This pattern appears to be controlled by the initiation and growth of ablation hollows in snow, until they reach a self-limiting condition, which in turn may be controlled by solar elevation angle, snow dust content or the magnitude of the turbulent fluxes.

Temporal snow  $z_0$  variation may be successfully explained by independent variables which accumulate from the time of the last snowfall: melt, daily maximum temperature and incoming shortwave radiation, and days. Parameterizations based on accumulated melt and accumulated daily maximum temperature can also account for along glacier spatial  $z_0$  variations. Non-linear relationships,

which model the variable rate of snow  $z_0$  increase over the ablation season, explain >80% of  $z_0$  variation (Fig. 7). [AUTHOR: Does the '>80%' figure need further justification, as it is not mentioned earlier? Also it appears in the abstract, so it seems an important finding.]

Patterns of ice  $z_0$  variation at Haut Glacier d'Arolla were less systematic than those for snow. Locally, some marked spatial patterns appeared, related to areas of rough or smooth ice (possibly a function of ice flow and foliation bands) and debris cover, which persisted from one season to the next. Temporally,  $z_0$  increased over some areas of the glacier during the first half of the ablation season and decreased slightly towards the season's end, but in other areas different temporal trends occurred. Consequently, it was not possible to explain ice  $z_0$  variation in terms of any independent variables.

The  $z_0$  of fresh, shallow snowfalls is strongly controlled by the underlying roughness elements. Variation of snow  $z_0$  following fresh snowfalls on ice, or rough snow, surfaces can be parameterized separately from 'deep' snow in a numerical melt model.

### 7.3. Implications for numerical melt models and future studies

The lack of a suitable parameterization scheme for glacier  $z_0$  variations has been widely acknowledged as a problem in the physically based modelling of glacier surface melt rates (Braithwaite, 1995; Hock and Holmgren, 1996; Hock and Noetzi, 1997; Samuelsson and others, 2003). The parameterizations developed here should improve the accuracy of turbulent flux calculations in energy balance models. The snow  $z_0$  parameterizations calculate an increase in snow  $z_0$  of three orders of magnitude between the early and mid-ablation season (or following a midsummer snowfall), which results in more than a doubling of the turbulent fluxes. This form of snow  $z_0$  variation (Fig. 7) implies glacier snow melt models must accommodate a step change in the rate of turbulent heat transfer to melting snow if they are to accurately calculate the time of underlying ice exposure. The temporal pattern of  $z_0$  variation on melting snow, and its causes, demands further investigation. The errors in turbulent flux calculations resulting from the use of a constant mean ice  $z_0$  are relatively small, due to the smaller range of variation of ice  $z_0$  than snow  $z_0$ . Based on a mean  $z_0$  of 2.24 mm, variation of  $z_0$  in the one standard deviation range (of 0.92 to 5.46 mm) alters the turbulent fluxes by at most  $\pm 20\%$ .

The transferability of the snow  $z_0$  parameterization should be tested at other sites. The size to which snow ablation hollows grow is controlled by local environmental factors such as insolation and snow dust content (Hunt, 1993), thus parameter values in the snow  $z_0$  parameterization may differ between regions with factors such as latitude and proximity to sources of dust and soot. Further study of ice  $z_0$  on different glaciers is warranted, particularly if such work aims to identify characteristic ice  $z_0$  types, which may be usefully incorporated into numerical melt models. Given that areas of debris, and areas of rough ice controlled by dynamics and foliation bands, tend to persist, a single microtopographic survey of a glacier could be used to generate a map of the spatial variation of  $z_0$  for use in a distributed melt model. There is evidence from this study that areas of relatively rough, or smooth, ice are preserved from one year to the next. Mapping areas of ice  $z_0$  is time consuming, even using

microtopographic methods, so the application of radar from satellite, airborne or ground-based platforms to glacier  $z_0$  measurements should be investigated.

### ACKNOWLEDGEMENTS

This work was supported by NERC Studentship GT4/92/5/P to B. Brock, with additional funding from NERC Grant GT3/8114. The weather stations were borrowed from the NERC equipment pool and anemometers and a wind vane were loaned by the British Antarctic Survey. We would like to thank P. Anderson of BAS for his help with the wind profile measurement set up; the members of the 1992–1994 Arolla Glaciology Project, in particular B. Hubbard, M. Nielsen and the Cambridge University undergraduates who helped with the fieldwork; Grande Dixence SA, Y. Bams, P. and B. Bourneis and M.V. Anzevui for their logistical assistance and J. Ford for cartographical assistance with Figure 1. The helpful comments of S. Munro, two anonymous reviewers and scientific editors R. Hock and M. Van den Broeke on previous versions of this paper are gratefully acknowledged.

### REFERENCES

- Ambach, W. 1963. Untersuchungen zum Energieumsatz in der Ablationszone des Grönländischen Inlandeises. *Medd. Grönl.*, **174**(4). Expédition Glaciologique Internationale au Groenland, E.G.I.G., 1957–1960, 4(4).
- Ambach, W. 1977. Untersuchungen zum Energieumsatz in der Akkumulationszone des grönländischen Inlandeises. *Medd. Grönl.*, **187**(7). Expédition Glaciologique Internationale au Groenland, E.G.I.G., 1967–1968, 4(7). [AUTHOR: please confirm this is the ref you intended]
- Andreas, E.L. 1987. A theory for the scalar roughness and the scalar transfer coefficients over snow and sea ice. *Bound. -Lay. Meteorol.*, **38**(1–2), 159–184.
- Andreas, E.L. 2002. Parameterizing scalar transfer over snow and ice: a review. *J. Hydrometeorology*, **3**(4), 417–432.
- Arck, M. and D. Scherer. 2002. Problems in the determination of sensible heat flux over snow. *Geogr. Ann.*, **84A**(3–4), 157–169.
- Arnold, N.S., I.C. Willis, M.J. Sharp, K.S. Richards and W.J. Lawson. 1996. A distributed surface energy-balance model for a small valley glacier. I. Development and testing for Haut Glacier d'Arolla, Valais, Switzerland. *J. Glaciol.*, **42**(140), 77–89.
- Arnold, N.S. and W.G. Rees. 2003. Self-similarity in glacier surface characteristics. *J. Glaciol.*, **49**(167), 547–554.
- Bintanja, R. 2000. The surface heat budget of Antarctic snow and blue ice: interpretation of temporal and spatial variability. *J. Geophys. Res.*, **105**(D19), 24,387–24,407.
- Bintanja, R. 2001. Characteristics of snowdrift over a bare ice surface in Antarctica. *J. Geophys. Res.*, **106**(D9), 9653–9659.
- Bintanja, R. and M.R. Van den Broeke. 1994. Local climate, circulation and surface-energy balance of an Antarctic blue-ice area. *Ann. Glaciol.*, **20**, 160–168.
- Bintanja, R. and M.R. Van den Broeke. 1995. The surface energy balance of Antarctic snow and blue ice. *J. Appl. Meteorol.*, **34**(4), 902–926.
- Braithwaite, R.J. 1995. Aerodynamic stability and turbulent sensible-heat flux over a melting ice surface, the Greenland ice sheet. *J. Glaciol.*, **41**(139), 562–571.
- Brock, B.W., I.C. Willis, M.J. Sharp and N.S. Arnold. 2000. Modelling seasonal and spatial variations in the surface energy balance of Haut Glacier d'Arolla, Switzerland. *Ann. Glaciol.*, **31**, 53–62.

- Brutsaert, W. 1975. A theory of local evaporation (or heat transfer) from rough and smooth surfaces at ground level. *Water Resour. Res.*, **11**, 543–550.
- Denby, B. and W. Greuell. 2000. The use of bulk and profile methods for determining surface heat fluxes in the presence of glacier winds. *J. Glaciol.*, **46**(154), 445–452.
- Denby, B. and P. Smeets. 2000. Derivation of turbulent flux profiles and roughness lengths from katabatic flow dynamics. *J. Appl. Meteorol.*, **39**(9), 1601–1612. (10.1175/1520-0450(2000)039.1601.)
- Denby, B. and H. Snellen. 2002. A comparison of surface renewal theory with the observed roughness length for temperature on a melting glacier surface. *Bound. -Lay. Meteorol.*, **103**(3), 459–468.
- Duynkerke, P.G. and M.R. Van den Broeke. 1994. Surface energy balance and katabatic flow over glacier and tundra during GIMEX-91. *Global Planet. Change*, **9**(1–2), 17–28.
- Föhn, P.M.B. 1973. Short-term snow melt and ablation derived from heat- and mass-balance measurements. *J. Glaciol.*, **12**(65), 275–289.
- Garratt, J.R. 1992. *The atmospheric boundary layer*. Cambridge, Cambridge University Press.
- Georges, C. and G. Kaser. 2002. Ventilated and unventilated air temperature measurements for glacier-climate studies on a tropical high mountain site. *J. Geophys. Res.*, **107**(D24). (10.1029/2002JD002503.)
- Goodsell, B., M.J. Hambrey, N.F. Glasser, P. Nienow and D. Mair. 2003. The structural glaciology of a temperate valley glacier: Haut Glacier d'Arolla, Valais, Switzerland. *Arct. Antarct. Alp. Res.*, **37**(2), 218–232.
- Grainger, M.E. and H. Lister. 1966. Wind speed, stability and eddy viscosity over melting ice surfaces. *J. Glaciol.*, **6**(43), 101–127.
- Greuell, W., W.H. Knap and P.C. Smeets. 1997. Elevational changes in meteorological variables along a mid-latitude glacier during summer. *J. Geophys. Res.*, **102**(D22), 25,941–25,954.
- Greuell, W. and P. Smeets. 2001. Variations with elevation in the surface energy balance on the Pasterze (Austria). *J. Geophys. Res.*, **106**(D23), 31,717–31,727.
- Greuell, W. and C. Genthon. 2004. Modelling land-ice surface mass balance. In Bamber, J. L. and A.J. Payne, eds. *Mass balance of the cryosphere: observations and modelling of contemporary and future changes*. Cambridge, Cambridge University Press.
- Grönlund, A., D. Nilsson, I.K. Koponen, A. Virkkula and M.E. Hansson. 2002. Aerosol dry deposition measured with eddy-covariance technique at Wasa and Aboa, Dronning Maud Land, Antarctica. *Ann. Glaciol.*, **35**, 355–361.
- Havens, J.M., F. Müller and G.C. Wilmot. 1965. Comparative meteorological survey and a short-term heat balance study of the White Glacier, Canadian Arctic Archipelago – summer 1962, Axel Heiberg Island Research Reports. Meteorology 4. Montréal, Que, McGill University.
- Hay, J.E. and B.B. Fitzharris. 1988. A comparison of the energy-balance and bulk-aerodynamic approaches for estimating glacier melt. *J. Glaciol.*, **34**(117), 145–153.
- Hock, R. and B. Holmgren. 1996. Some aspects of energy balance and ablation of Storglaciären, northern Sweden. *Geogr. Ann.*, **78A**(2–3), 121–131.
- Hock, R. and C. Noetzli. 1997. Areal melt and discharge modelling of Storglaciären, Sweden. *Ann. Glaciol.*, **24**, 211–216.
- Hogg, I.G.G., J.G. Paren and R.J. Timmis. 1982. Summer heat and ice balances on Hodges Glacier, South Georgia, Falkland Islands Dependencies. *J. Glaciol.*, **28**(99), 221–238.
- Högström, U. 1988. Non-dimensional wind and temperature profiles in the atmospheric surface layer: a re-evaluation. *Bound. -Lay. Meteorol.*, **42**(1–2), 55–78.
- Hoinkes, H. 1953. Wärmeumsatz und Ablation auf Alpengletschern. II: Hornkees (Zillertaler Alpen), September 1951. *Geogr. Ann.*, **35**(2), 116–140.
- Hoinkes, H. and N. Untersteiner. 1952. Wärmeumsatz und Ablation auf Alpengletschern. I: Vernagtferner (Ötztaler Alpen), August 1950. *Geogr. Ann.*, **34**(1–2), 99–158.
- Holmgren, B. 1971. Climate and energy exchange on a sub-polar ice cap in summer. Arctic Institute of North America Devon Island Expedition 1961–1963. Part E. Radiation climate, Meddelande. 111. Uppsala, Uppsala Universitet. Meteorologiska Institutionen.
- Hunt, J.B. 1993. Correspondence. Ablation thresholds and ash thickness. *J. Glaciol.*, **39**(133), 705–707.
- Inoue, J. 1989. Surface drag over the snow surface of the Antarctic Plateau. 1. Factors controlling surface drag over the katabatic wind region. *J. Geophys. Res.*, **94**(D2), 2207–2217.
- Ishikawa, N., I.F. Owens and A.P. Sturman. 1992. Heat balance characteristics during fine periods on the lower part of the Franz Josef Glacier, S. Westland, New Zealand. *Int. J. Climatol.*, **12**, 397–410.
- Jackson, B.S. and J.J. Carroll. 1978. Aerodynamic roughness as a function of wind direction over asymmetric surface elements. *Bound. -Lay. Meteorol.*, **14**, 323–330.
- Keeler, C.M. 1964. Relationship between climate, ablation, and run-off on the Sverdrup Glacier, 1963, Devon island, N.W.T, AINA Research Paper. 27. Montréal (Quebec), Arctic Institute of North America.
- King, J.C. 1990. Some measurements of turbulence over an Antarctic ice shelf. *Q. J. Roy. Meteor. Soc.*, **116**(492), 379–400.
- King, J.C. and P.S. Anderson. 1994. Heat and water vapour fluxes and scalar roughness lengths over an Antarctic ice shelf. *Bound. -Lay. Meteorol.*, **69**(1–2), 101–121.
- Klok, E.J. and J. Oerlemans. 2002. Model study of the spatial distribution of the energy and mass balance of Morteratschglletscher, Switzerland. *J. Glaciol.*, **48**(163), 505–518.
- Lettau, H. 1969. Note on aerodynamic roughness-parameter estimation on the basis of roughness element description. *J. Appl. Meteorol.*, **8**(5), 828–832.
- Liljequist, G.H. 1954. Radiation and wind and temperature profiles over an Antarctic snowfield – a preliminary note. In *Proceedings, Meteorological Conference, Toronto, Ontario*. American Meteorological Society; Royal Meteorological Society, 78–87.
- Mair, D., P. Nienow, M. Sharp, T. Wohlleben and I. Willis. 2002. Influence of subglacial drainage system evolution on glacier surface motion: Haut Glacier d'Arolla, Switzerland. *J. Geophys. Res.*, **107**(B8). (10.1029/2001JB000514.)
- Martin, S. 1975. Wind regimes and heat exchange on Glacier de Saint-Sorlin. *J. Glaciol.*, **14**(70), 91–105.
- Meesters, A., N. Bink, H.F. Vugts, F. Cannemeijer and E. Henneken. 1997. Turbulence observations above a smooth melting surface on the Greenland ice sheet. *Bound. -Lay. Meteorol.*, **85**, 81–110.
- Moore, R.D. and I.F. Owens. 1984. Controls on advective snowmelt in a maritime alpine basin. *J. Climate Appl. Meteorol.*, **23**(1), 135–142.
- Morris, E. 1989. Turbulent transfer over snow and ice. *J. Hydrol.*, **105**, 205–223.
- Munro, D.S. 1989. Surface roughness and bulk heat transfer on a glacier: comparison with eddy correlation. *J. Glaciol.*, **35**(121), 343–348.
- Munro, D.S. 1990. Comparison of melt energy computations and ablatometer measurements on melting ice and snow. *Arct. Alp. Res.*, **22**(2), 153–162.
- Munro, D.S. and J.A. Davies. 1977. An experimental study of the glacier boundary layer over melting ice. *J. Glaciol.*, **18**(80), 425–436.
- Obleitner, F. 2000. The energy budget of snow and ice at Breidamerkurjökull, Vatnajökull, Iceland. *Bound. -Lay. Meteorol.*, **97**(3), 385–410.
- Oerlemans, J. 2001. *Glaciers and climate change: a meteorologist's view*, Lisse, Netherlands, A.A. Balkema.
- Oke, T.R. 1987. *Boundary layer climates*, Second edition. London, Routledge Press.



- Paterson, W.S.B. 1994. *The physics of glaciers, Third edition*. Oxford, Elsevier.
- Plüss, C. and R. Mazzoni. 1994. The role of turbulent heat fluxes in the energy balance of high Alpine snow cover. *Nord. Hydrol.*, **25**(1–2), 25–38.
- Poggi, A. 1976. Heat balance in the ablation area of the Ampere Glacier (Kerguelen Islands). *J. Appl. Meteorol.*, **16**, 48–55.
- Price, A.G. 1977. *Snowmelt runoff processes in a subarctic area, McGill Sub-Arctic Research Paper 29*. Climatological Research Series 10. Montréal, Que., McGill University. Department of Geography.
- Richards, K.S. and 9 others. 1996. An integrated approach to modelling hydrology and water quality in glacierized catchments. *Hydrol. Process.*, **10**, 479–508.
- Samuelsson, P., B. Bringfelt and L.P. Graham. 2003. The role of aerodynamic roughness for runoff and snow evaporation in land-surface schemes – comparison of uncoupled and coupled simulations. *Global Planet. Change*, **38**(1–2), 93–99.
- Schneider, C. 1999. Energy balance estimates during the summer season of glaciers of the Antarctic Peninsula. *Global Planet. Change*, **22**(1–4), 117–130.
- Skieb, G. 1962. Zum Stahlungs- und Wärmehaushalt des Zentralen Tjuksu-Gletschers im Tienschan-Gebirge. *Zeitschrift für Meteorologie*, **16**(1), 1–9.
- Smeets, C.J.P.P., P.G. Duynkerke and H.F. Vugts. 1998. Turbulence characteristics of the stable boundary layer over a mid-latitude glacier. Part II. Pure katabatic forcing conditions. *Bound. -Lay. Meteorol.*, **87**(1), 117–145.
- Smeets, C.J.P.P., P.G. Duynkerke and H.F. Vugts. 1999. Observed wind profiles and turbulence fluxes over an ice surface with changing surface roughness. *Bound. -Lay. Meteorol.*, **92**(1), 101–123.
- Strasser, U., J. Corripio, F. Pellicciotti, P. Burlando, B. Brock and M. Funk. 2004. Spatial and temporal variability of meteorological variables at Haut Glacier d'Arolla (Switzerland) during the ablation season 2001: measurements and simulations. *J. Geophys. Res. -Atmos.*, **109**(D3), 3103–3103.
- Streten, N.A. and G. Wendler. 1968. The midsummer heat balance of an Alaskan maritime glacier. *J. Glaciol.*, **7**(51), 431–440.
- Stull, R.B. 1988. *An introduction to boundary layer meteorology*, Dordrecht, etc., Kluwer Academic Publishers.
- Sverdrup, H.U. 1936. The eddy conductivity of the air over a smooth snow field. Results of the Norwegian-Swedish Spitsbergen Expedition in 1934. *Geofysiske Publikasjoner*, **11**(7), 1–69.
- UNIRAS. 1990. *Unimap 2000 user's manual. Version 6*, Søborg, Denmark, UNIRAS Ltd.
- Untersteiner, N. 1957. Glazial-meteorologische Untersuchungen im Karakorum. II: Wärmehaushalt. *Arch. Meteorol. Geophys. Bioklimatol., (B)*, **8**(2), 137–171.
- Van de Wal, R.S.W., J. Oerlemans and J.C. van der Hage. 1992. A study of ablation variations on the tongue of Hintereisferner, Austrian Alps. *J. Glaciol.*, **38**(130), 319–324.
- Van de Wal, R.S.W. and A.J. Russell. 1994. A comparison of energy balance calculations, measured ablation and meltwater runoff near Søndre Strømfjord, West Greenland. *Global Planet. Change*, **9**(1–2), 29–38.
- Wagnon, P., P. Ribstein, G. Kaser and P. Berton. 1999. Energy balance and runoff seasonality of a Bolivian glacier. *Global Planet. Change*, **22**(1–4), 49–58.
- Wendler, G. and N.A. Streten. 1969. A short term heat balance study on a coast range glacier. *Pure and Applied Geophysics (PAGEOPH)*, **77**, 68–77.
- Wendler, G. and G. Weller. 1974. A heat-balance study on McCall Glacier, Brooks Range, Alaska: a contribution to the International Hydrological Decade. *J. Glaciol.*, **13**(67), 13–26.
- Wieringa, J. 1993. Representative roughness parameters for homogeneous terrain. *Bound. -Lay. Meteorol.*, **63**(4), 323–363.
- Willis, I., N. Arnold and B. Brock. 2002. Effect of snowpack removal on energy balance, melt and runoff in a small supraglacial catchment. *Hydrol. Process.*, **16**(14), 2721–2749.

MS received 16 August 2005 and accepted in revised form 4 May 2006